

## INNOVATIONS IN LIFE SCIENCE RESEARCH

IN CONVERSATION WITH **MR. HARISH KUNDAPURA,**  
**VP, LIFE SCIENCES DIV., INKARP INSTRUMENTS**

CELEBRATING **MR. S. BALU'S**  
**(CMD, INKARP GROUP)**  
**LIFETIME ACHIEVEMENT AWARD**



Indian Analytical  
Instruments Association



## 39<sup>+</sup> Years

of Pioneering the Scientific Frontier

**Inkarp, established in 1985, honors 39 years** of dedication to the scientific community in India. Our journey continues to be driven by the pursuit of excellence in **offering cutting-edge scientific research instruments**. We take pride in providing scientists across the country with tools that facilitate discoveries and innovation.



**Scan**  
*to view our website*

Follow Us On





## From the editor

Dear Readers,

I'm excited to bring to you this new edition of CatalystCue. In this issue, we've explored some fascinating areas of science that I believe will resonate with many of you. Our cover story focuses on imaging-based biomarker detection—a topic that holds so much potential for changing the way we diagnose and treat diseases.

In this edition's feature, we discuss the challenges and progress in life sciences, particularly how technology is evolving to meet the demands of modern research. We also feature an insightful interview with Mr. Harish Kundapura, Vice President of Life Sciences Division at Inkarp Instruments. Mr. Harish shares his extensive experience in laboratory automation and liquid handling, shedding light on how advancements in these areas are revolutionizing life sciences research. He discusses the integration of automation in processes such as sample preparation, which enhances precision, efficiency, and reproducibility, while also addressing the challenges of long-term sample storage through innovations in biobanking. His insights underscore the evolving role of technology in supporting modern research demands across various fields, from genomics to cancer research.

The application showcase covers a range of interesting topics, from genetic breakthroughs in cancer research to innovative methods for studying viruses on the nanoscale. There's a detailed look at how siRNA delivery systems are being developed for more effective cancer treatments and how advanced imaging techniques are being used to assess drug responses. We've also touched on new ways to explore cell-based biopsies and tissue imaging, which are pushing research forward in exciting ways. For those interested in agricultural science, we've included a method for determining protein content in soybeans that could be of great value.

Our technical corner offers practical advice on optimizing Western blot analysis, a technique many of you will find helpful in the lab. We've also highlighted a new approach to studying biomolecular interactions that I think will catch your attention. In the Industry Buzz section, we continue our regular updates on the latest FDA-approved drugs, this time with a new set making waves. You'll also find a preview of some exciting upcoming events in the world of science.

On a special note, we are proud to share that our Chairman and Managing Director, Mr. S. Balu, has recently been honoured with the Lifetime Achievement Award by the Indian Analytical Instruments Association (IAIA). This recognition is a proud moment for all of us at Inkarp and a testament to his remarkable contributions to the industry.

I hope this edition offers you something new to think about, whether you're looking for inspiration in your work or simply want to stay updated on the latest developments. As always, your feedback is important to us, and I look forward to hearing your thoughts.

Best regards,

Arun Mathrootham  
Director  
Inkarp Instruments Pvt. Ltd.

OCTOBER 2024

Volume 01      Issue 02

# Contents

## Cover Story

- 02 The Promise of Imaging-based Biomarker Validation in Cancer Research

## Features

- 06 Overview of the 2024 Nobel Prize in Physiology and Medicine.
- 08 In conversation with Mr. Harish Kundapura, Vice President, Life Sciences Division, Inkarp Instruments

## Application Showcase

- 10 Uncovering genetic clues to breast cancer chemo response with Implen Nanophotometer
- 13 Fighting viruses on the nanoscale with AFM using the Nanosurf Drive AFM
- 17 Efficient siRNA delivery to TNBC cells using polymer - lipid nanocomplexes utilising the Precision X-Ray Imaging
- 20 Native and staining-free pharmacologic assessment of drug dose responses using anvajo fluidlab R-300 - Cell Counter & Spectrometer
- 24 Exploring cell-based liquid biopsy: beyond circulating tumour cell enumeration - Utilising RareCyte platform
- 28 Inkarp's proud moments- Honouring Excellence: Mr. S. Balu, Chairman – Managing Director, Receives Lifetime Achievement Award from the Indian Analytical Instruments Association
- 30 Detailed description of Tissue Section Imaging with LICORbio's Odyssey® Imagers
- 37 Exploring applications of in vivo NIR-II imaging in preclinical research with Photon Etc IR VIVO NIR II Preclinical Imager
- 42 Determination of protein content in soybeans by Kjeldahl method employing the BEING BPK-9870A Automatic Kjeldahl Nitrogen Analyzer

## Tech Corner

- 45 Protocol: Quantitative Western Blot Analysis with replicate samples by LICORbio

## Product Highlight

- 50 Affinité Instruments: Surface Plasmon Resonance- Introducing Lensless SPR® Technology

## Industry Buzz

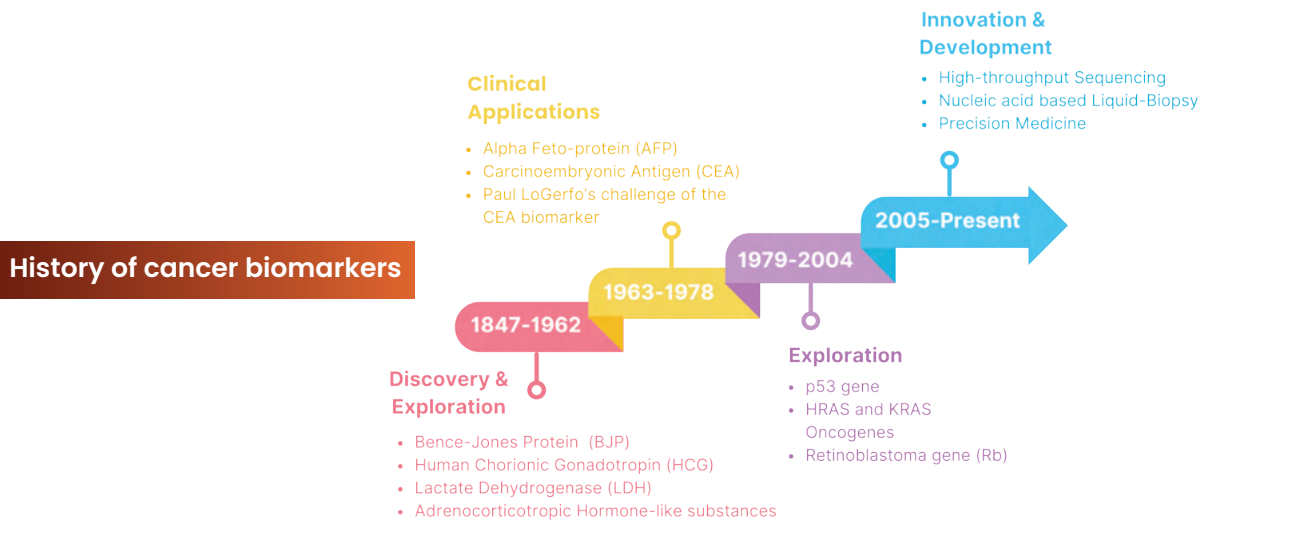
- 53 Rx updates: Recent novel FDA approved drugs
- 54 Sneak-peak at our events

## Early detection, early intervention – The Promise of Imaging-based Biomarker Validation in Cancer Research

**A**mong non-communicable diseases, cancer ranks second in the list of top causes of mortalities. The cancer burden is expected to rise to a shocking 29.8 million DALYs (adjusted mortality to incidence) in 2025 – and this is just the projected rate for India! Cancer mortality is seen to decrease substantially when detected in the early stages. An early diagnosis and screening can result in greater probability of survival, decreased cancer mortality, and not to mention, lower treatment costs. Early diagnosis of cancer is largely attributed to awareness and timely evaluation of diagnostic services. Screening, on the other hand, aims to identify individuals before they show symptoms of a specific cancer.

A biomarker is a measurable characteristic of the body that can indicate a normal process, condition or disease as a response to therapeutic intervention. A cancer biomarker is any biochemical entity which helps identify the increasing risk of developing cancer. These biomarkers may include lipids, small molecules, proteins, whole cells, nucleic acids etc.

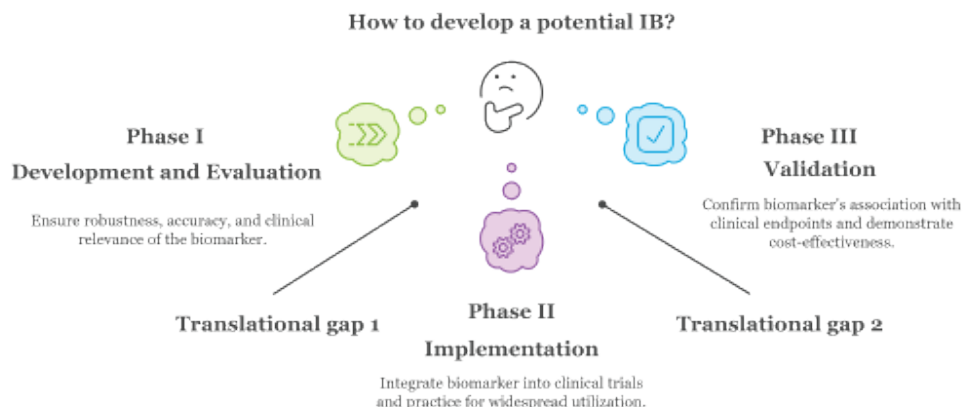
Detection of cancer biomarkers can be accomplished by a wide variety of tools. This article gives a glance at the developments and current trends in image-based biomarker validation for cancer research.



# Cover Story

With advancements in technology, the quest for biomarkers has been on the rise. Many biomarkers identified in laboratory settings have unfortunately failed to translate into clinically meaningful applications, highlighting the need for more comprehensive and integrative approaches to biomarker validation.

There are 2 translational barriers that all biomarkers must cross to be even considered as guides in clinical decisions. Crossing the first translational gap establishes the biomarker as a reliable medical tool. The second translational gap places biomarkers at the forefront of clinical decision-making.



## Imaging biomarkers have 4 key attributes-

- » They are a part of all biomarkers.
- » They may be quantitative or qualitative in nature.
- » Though all imaging biomarkers stem from various imaging modalities, each contributes as a distinct unit.
- » A single imaging measurement is capable of supporting multiple imaging biomarkers.

IBs provide ways of accessible and affordable, non-invasive screening and early detection of tumours as well as monitoring the patient on an ongoing basis. Some of these include assessment of treatment response and possible side effects.

IBs have developed the ability to repeatedly evaluate the same tumour in time, map the variation within tumours, and assess multiple lesions in one patient independently.

## Non-invasive imaging modalities for cancer biomarker validation

Imaging techniques provide non-invasive means to detect and assess tumour characteristics, identify biomarkers and evaluate treatment response. By utilising contrast agents or specific molecular probes, imaging modalities can visualise the expression or distribution of biomarkers within tissues and organs.

A variety of imaging modalities can be used for biomarker validation, each with its own advantages and limitations.

1. **Magnetic Resonance Imaging (MRI):** MRI is excellent for soft tissue contrast and can be used with contrast agents to make sure that certain biomarkers are better seen. Both DWI and PWI can be applied to assess the features of the tumour and its microenvironment.

# Cover Story

- 2. Computed Tomography (CT):** Another scan that CT offers would be to provide highly detailed pictures for better resolution. CT scans can be combined with certain contrast agents and detect altered blood flow and tissue density that characterizes cancer.
- 3. Positron Emission Tomography (PET):** PET utilizes radiotracers that release positrons to construct images from metabolic activities. By the application of specific biomarkers, PET may identify regions in which cellular growth or heightened metabolic activity could be associated with cancer.
- 4. Single-Photon Emission Computed Tomography (SPECT):** This is similar to PET, but the radiotracers give off gamma rays and have an application mainly in bone scans and sometimes in biomarker detection for various cancers.
- 5. Ultrasound:** The ultrasound imaging technique gives image through sound waves, which pass through tissues and organs. The use of ultrasonography is mainly anatomical visualization, but Doppler ultrasound can examine blood flow within the tumour.
- 6. Optical imaging:** Optical imaging has emerged as a powerful tool, possessing several advantages over the traditional imaging modalities. Key techniques include-
- » **Fluorescence imaging:** This technique involves the use of fluorescent probes that bind to specific biomarkers. When excited by appropriate light, these probes emit fluorescence, allowing for visualization of the target biomarker.
  - » **Bioluminescence imaging:** This technique relies on the detection of light emitted by bioluminescent proteins or enzymes expressed by cells or tumours. Bioluminescence imaging can be used to monitor the growth and spread of cancer cells *in vivo*.
  - » **Hyperspectral imaging:** This technique captures images across a wide range of wavelengths, allowing for the identification of specific biomarkers based on their unique spectral signatures.
  - » **Optical coherence tomography (OCT):** OCT provides high-resolution images of tissue microstructure, enabling the detection of early-stage cancer and the assessment of tumour heterogeneity.

Biomarker	Modality	Function
<i>IBs which have crossed translational gap 1 into therapeutic trials and hypothesis-driven research</i>		
Left ventricular ejection fraction	Scintigraphy, US	Safety biomarker, Guides decision to stop therapy
AUC	US	Pharmacodynamic and putative predictive IB
<sup>18</sup> F-FDG SUV <sub>max</sub>	PET	For regional selective dose boost
ΔK <sup>trans</sup> (and related IBs)	CT, MRI	Proof-of-concept, Used for dose-finding, Informs go/no-go decision-making on the basis of biologically active dose versus MTD, Used for dose-scheduling

# Cover Story

Biomarker	Modality	Function
<i>IBs that have crossed translational gap 2 into healthcare</i>		
Clinical TNM stage	XR, CT, MRI, PET, SPECT, US, endoscopy	Prognostic in almost all cancers
Bone scan index	SPECT	Prognostic in prostate cancer
Uptake of <sup>111</sup> Inpentetetreotide, <sup>68</sup> Ga-dotatate octreotide conjugates	SPECT, PET	Identification of primary or residual neuroendocrine lesions, Prescription of <sup>177</sup> Lu-dotatateoctreotide ablation therapy
Objective response	CT, MRI, PET	Guides decision to continue, discontinue, or switch therapy
<i>IBs approved by FDA as surrogate end points</i>		
Objective response	CT, MRI, PET	End point in phase II trials, Contribution to PFS determination
Splenic Volume	CT, MRI	Assessments of response in patients with myelofibrosis

Table 1: Few illustrative examples of image-based biomarkers in various cancer types

## Conclusion

Biomarkers detected using the strength of imaging technology help researchers and clinicians identify those that aid in the early detection, correct diagnosis, and proper staging of cancer. Such biomarkers also provide information that proves invaluable in terms of prognosis, response to treatment, and monitoring for recurrence. With ever-advancing technology, and particularly with imaging combined with biomarker detection, it is well poised to be part of a strategy that would improve patient outcomes and change the landscape of cancer care.

## References

1. O'Connor, J. P. B.; Aboagye, E. O.; Adams, J. E.; Aerts, H. J. W. L.; Barrington, S. F.; Beer, A. J.; Boellaard, R.; Bohndiek, S. E.; Brady, M.; Brown, G.; Buckley, D. L.; Chenevert, T. L.; Clarke, L. P.; Collette, S.; Cook, G. J.; deSouza, N. M.; Dickson, J. C.; Dive, C.; Evelhoch, J. L.; Faivre-Finn, C. Imaging Biomarker Roadmap for Cancer Studies. *Nature Reviews Clinical Oncology* 2017, 14 (3), 169–186. DOI: 10.1038/nrclinonc.2016.162.
2. Bernsen, M. R.; Kooiman, K.; Segbers, M.; van Leeuwen, F. W. B.; de Jong, M. Biomarkers in Preclinical Cancer Imaging. *European Journal of Nuclear Medicine and Molecular Imaging* 2015, 42 (4), 579–596. DOI: 10.1007/s00259-014-2980-7.
3. Winfield, J. M.; Payne, G. S.; deSouza, N. M. Functional MRI and CT Biomarkers in Oncology. *European Journal of Nuclear Medicine and Molecular Imaging* 2015, 42 (4), 562–578. DOI: 10.1007/s00259-014-2979-0.
4. Pien, H. H.; Fischman, A. J.; Thrall, J. H.; Sorensen, A. Gregory. Using Imaging Biomarkers to Accelerate Drug Development and Clinical Trials. *Drug Discovery Today* 2005, 10 (4), 259–266. DOI: 10.1016/s1359-6446(04)03334-3.

# VCX 750

A powerful and versatile ultrasonic liquid processor



**SONICS®**  
SONICS & MATERIALS, INC.



Accessorize and customise according to your application

## FEATURES:

- 01 Microprocessor based
- 02 Programmable
- 03 Variable power output
- 04 10-hour timer
- 05 Pulse mode
- 06 Wattage and Energy display
- 07 Temperature monitoring
- 08 Energy setpoint

## The 2024 Nobel Prize in Physiology: Celebrating Victor Ambros and Gary Ruvkun's Pioneering Work on MicroRNAs

The 2024 Nobel Prize in Physiology or Medicine has been awarded to Victor Ambros and Gary Ruvkun for their groundbreaking discoveries in the field of microRNA research.

Victor Ambros joined the Horvitz lab at MIT, post his PhD, where he studied poliovirus genome structure. Here, he quickly turned his attention to *C. elegans*, investigating heterochronic mutations, characterised by defects in its developmental timing. He identified the lin-14 gene, which exhibited developmental timing defects opposite to those observed in the lin-4 mutant. In lin-14 mutants, it was observed that larval programs were absent entirely, marking a significant finding in the field of developmental genetics.

Gary Ruvkun, at the same time became interested in the genetic underpinnings of *C. elegans*, particularly in the cell lineage analyses of heterochronic mutants. Following discussions, Ruvkun joined forces with Ambros, marking the beginning of a fruitful collaboration.

The duo set out to clone the lin-14 gene. Identifying DNA sequences based on genetic information proved challenging, but after years of effort, they succeeded using restriction fragment length polymorphism (RFLP) techniques. They demonstrated that lin-14 is a nuclear protein with stage-specific expression, notably high during the L1 larval stage. Their investigations revealed that lin-14's regulation involved a post-transcriptional mechanism, particularly through the 3' untranslated region (3' UTR), a key insight that opened new avenues for understanding gene expression.

Simultaneously, Ambros's lab focused on identifying lin-4, the first microRNA. Through rigorous genomic analysis, they isolated the lin-4 gene, which was ultimately confirmed to be a non-coding RNA. The lab's findings revealed that lin-4 produced two short RNA

transcripts, measuring 61 and 22 nucleotides in length. On June 11, 1992, a pivotal moment occurred when Ambros and Ruvkun exchanged their sequences for lin-4 and lin-14, discovering complementary sequences that indicated a regulatory relationship. Their subsequent experiments confirmed that lin-4 microRNA regulates lin-14 mRNA by base pairing with its 3' UTR.

### Expanding the Understanding of MicroRNAs

The discovery of lin-4 laid the groundwork for understanding microRNAs as a new class of regulatory molecules. Following this, Ruvkun's lab identified the let-7 microRNA, seven years after the discovery of lin-4. Unlike lin-4, let-7 was evolutionarily conserved across various species, indicating a broader regulatory role in development.

The presence of let-7 across multiple organisms—from nematodes to humans—suggested a fundamental role in regulating gene expression during developmental transitions. It was shown to target several genes involved in developmental timing, further establishing microRNAs as key players in post-transcriptional regulation.

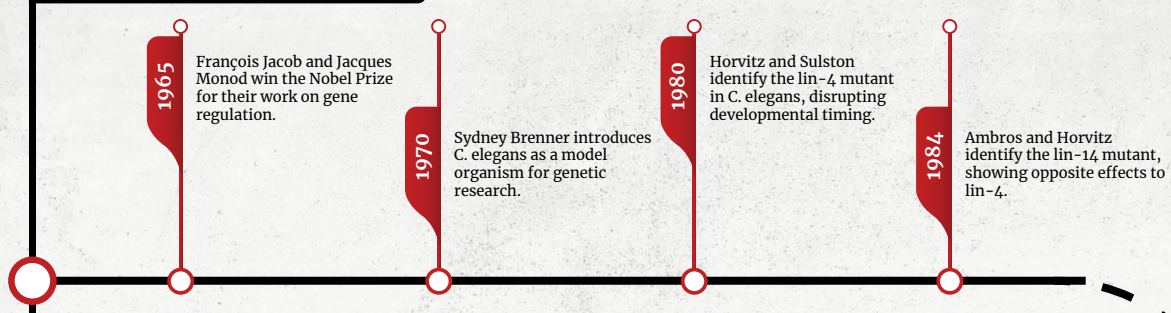
### Conclusion

The impact of Ambros and Ruvkun's work extends far beyond the initial discoveries of lin-4 and let-7. Since then, microRNAs have been identified across thousands of species, significantly advancing our understanding of gene regulation.

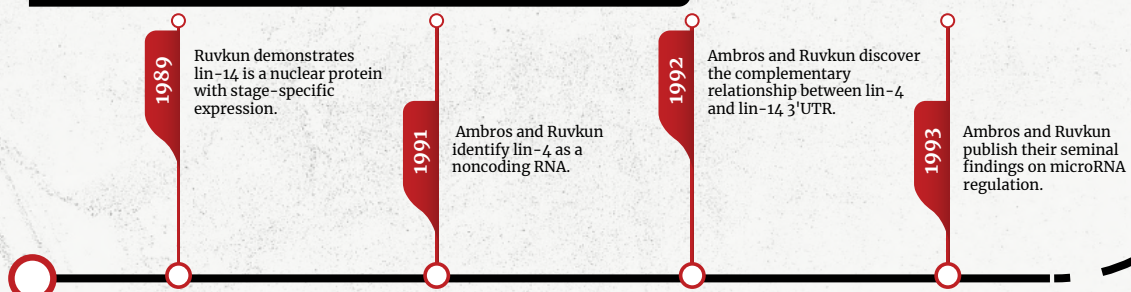
Recent advancements in sequencing technologies and computational analyses have illuminated the rules governing microRNA interactions with target mRNAs, providing insights into their regulatory mechanisms.

MicroRNAs have also been implicated in a wide range of biological processes, including development, cell differentiation, metabolism, and immune function. Dysregulation of microRNA expression has been linked to various human diseases, making them attractive targets for therapeutic intervention. This discovery of microRNA has paved the way for exciting research advancements.

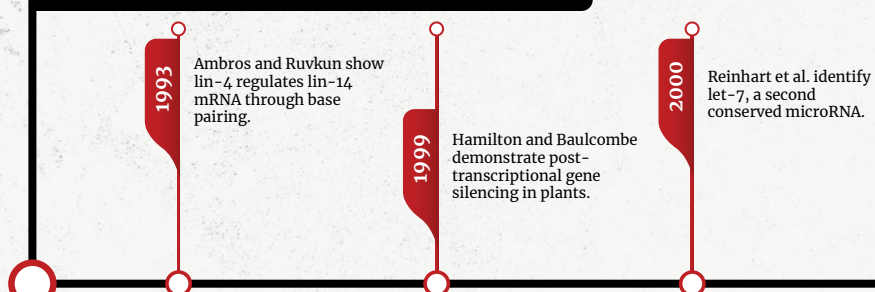
## Early Discoveries (1960s-1980s)



## Cloning and Characterization of MicroRNAs (1989-1993)



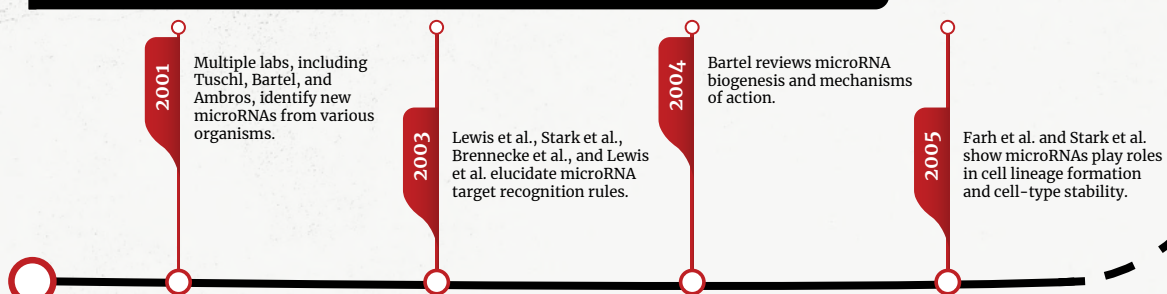
## Expansion of MicroRNA Research (1993-2000)



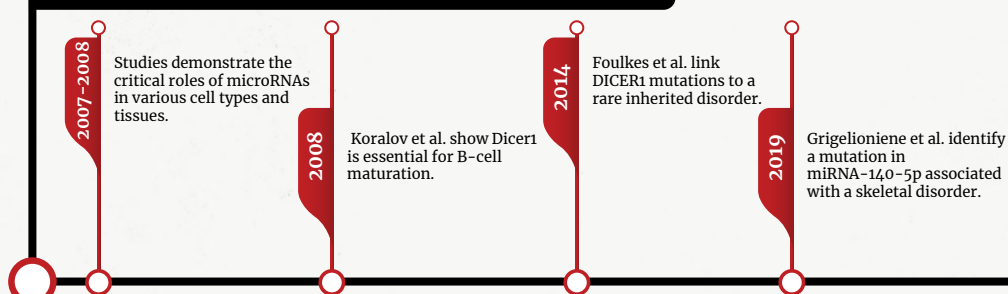
## Reference

The Nobel Prize in Physiology or Medicine 2024. NobelPrize.org. <https://www.nobelprize.org/prizes/-medicine/2024/advanced-information/>.

## Identification and Characterization of Additional MicroRNAs (2001-2005)



## MicroRNA Functions and Applications (2005-Present)



## Ongoing research

Continued efforts to understand microRNA functions, develop diagnostics, and therapeutics.



## Mr. Harish Kundapura

(Vice President, Life Sciences Division, Inkarp Instruments)

is a seasoned life sciences professional with a strong background in laboratory automation and screening. He has held key positions at renowned companies like Toshniwal Bros Bengaluru, Nulab Equipments, and Sartorius Biotech India. Currently leading the Life Sciences Division at Inkarp Instruments, Mr. Harish, along with his colleagues, have successfully executed large-scale projects like Automated Compound Management and Small Molecule Repository at CSIR-IICT, Hyderabad and CSIR-CDRI, Lucknow.

Presently, Mr. Harish is working on expanding into emerging areas like Cell & Gene Therapy and Spatial Biology. His expertise and passion for innovation make him an asset to the life sciences industry.

*Given your extensive experience in liquid handling and automation, what are some of the most significant advancements you've witnessed in this field over the years?*

HK: Automation in liquid handling has revolutionised the genomics research, NGS, drug discovery and recently liquid biopsy. Researchers can increase their efficiency, speed, reproducibility, throughput and reduce the human error.

*How has the integration of automation impacted the efficiency and reproducibility of life sciences research?*

HK: Yes. Not only efficiency and reproducibility but also the speed and accuracy. Pharma industries are required to produce results in a shorter period and integration of automation helps a lot. E.g., we have integrated automation for sample prep for compound management at CSIR-CDRI.

*How can one balance the need for precision and reproducibility in liquid handling with the demands for high throughput and scalability in modern research?*

HK: Precision, reproducibility and speed are the factors which play crucial role in high throughput labs. Scalability of course depends on the data you get.

*What are some of the emerging applications of liquid handling and automation technologies in life sciences, beyond traditional research settings?*

HK: Compound management and biobanking have become a standard method in life sciences research Good Laboratory Practice. Latest is in cancer research i.e. integration of automation and imaging for liquid biopsy samples. In fact, RareCyte is a company specialised in this field. Hawk Biosystems is a complimentary product to aid cancer research.

*How are biobanks addressing the challenges of long-term sample storage, such as degradation and contamination?*

HK: Temperature gradients must be controlled precisely. This is a challenging one due to the frequent power disruptions in India. Biobanks must have a facility to maintain the storage temperature even if there is power failure. Sample collection and handling of samples is very crucial in long term storage, especially the bio-samples used for medical and healthcare research. Contamination can be avoided by upgrading the storage to online integration of sample collection/transporting/handling (including the thawing).

# Interview

**What are the long-term costs and benefits of different sample storage methods?**

**HK:** With the advancements in automation of sample storage and retrieval, costs have significantly reduced. Organisations are saving lot of money by automation of sample handling and storage.

**With increase in the use of human biospecimens in research, what are your thoughts in ethical implications and data privacy?**

**HK:** Use of human biospecimens in storage is regulated. Data must be standardised and validated. Both biological data and clinical data. Transparent sharing of data is important.

**What are some of the most exciting technological advancements in the field of life sciences instrumentation?**

**HK:** It is to do with cells. How good you are in studies of cell science, in terms of sorting and image analysis of cells. AI has made the life of researchers easier. Of course, we have to be very careful while validating

the data. If my understanding is correct, laws are yet to be framed for use of the data generated by GenAI.

**What are the key factors driving growth or challenges in the market?**

**HK:** Life Sciences is a sector which has long incubation time. It is the life sciences analytics which will drive the growth. Again, as I stated earlier, analytical solutions will play an important role in this. The data generated by analytical solutions will help us to take preventive measures to counter the pricing pressure and geopolitical changes.

**How are changes in the regulatory landscape impacting research and development in the life sciences industry?**

**HK:** Regulatory laws are being modernized to keep pace with healthcare developments in vaccines and medicines. Post COVID, EU and US are putting in place the regulations to suit the present trend in the research and development.



CSIR-IICT, Hyderabad  
Installation of Universal Store  
Capacity: 1 million Samples



CSIR-CDRI, Lucknow  
Installation of LabStore  
Capacity: 600,000 samples and Automated Sample Prep/HT Screening Setup

## Uncovering genetic clues to breast cancer chemo response



### Nucleic acid quantification using Implen NanoPhotometer

**A**ccurate quantification of nucleic acids is crucial in cancer research for number of reasons. From detection and analysis of genetic alterations to monitoring treatment response, quantification of DNA, RNA and nucleic acids has its own role in advancing our comprehension of cancer research. This application sheds lights on the use of Implen NanoPhotometer in DNA and RNA quantification in the context of breast cancer research, focusing its role in understanding genomic changes, identifying biomarkers and developing targeted therapies.

**Keywords:** DNA, RNA, quantification, neoadjuvant chemotherapy, breast cancer, Implen NanoPhotometer

### Introduction

Neoadjuvant chemotherapy is a systematic pre-surgical treatment where chemotherapy is given before surgery for patients with localised high risk or inoperable tumours. Often used for breast cancer, it is aimed at downsizing the tumour to avoid axillary dissections in patients. Successful therapy paves way for preservation of organs, avoiding mastectomy, and reducing surgical dissections in sensitive patients. Although there are studies which indicate significant advantages of neoadjuvant chemotherapy, predicting its response is difficult due to tumour heterogeneity and limited precision of existing biomarkers. Therefore, the key goal remains achieving subsequent pathological complete response. To accomplish this, prediction of novel biomarkers by identifying patients who might benefit from neoadjuvant therapy.

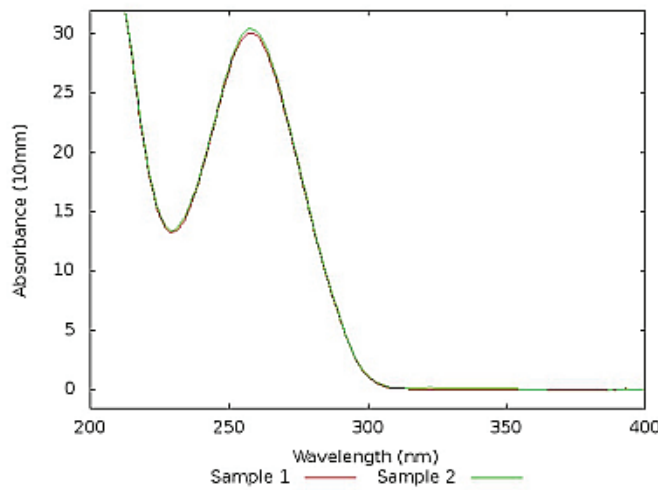
This application highlights the use of Implen NanoPhotometer® for the quantification of DNA and RNA.

# Application Showcase

## Parameter

Method	Nucleic Acids			Nucleic Acid Factor	40.00
Type	RNA			Background Correction	320 nm
Mode	NanoVolume			Air Bubble Recognition	Off
Volume (μl)	1-2			Manual Dilution Factor	1.000

#	Name	Conc.	Units	A230	A260	A280	A320	A260/A280	A260/A230	Dilution
1	Blank 1	0.0000	ng/μl	0.000	0.000	0.000	0.000	0.000	0.000	1.000
2	Sample 1	1195.3	ng/μl	13.29	29.89	14.02	0.008	2.133	2.250	140
3	Sample 2	1203.1	ng/μl	13.42	30.18	14.23	0.103	2.129	2.259	140



## Parameter

Method	Nucleic Acids			Nucleic Acid Factor	50.00
Type	dsDNA			Background Correction	320 nm
Mode	NanoVolume			Air Bubble Recognition	Off
Volume (μl)	1-2			Manual Dilution Factor	1.000

#	Name	Conc.	Units	A230	A260	A280	A320	A260/A280	A260/A230	Dilution
1	Blank 1	0.0000	ng/μl	0.000	0.000	0.000	0.000	0.000	0.000	1.000
2	Sample 1	795.20	ng/μl	6.993	15.90	8.405	-0.004	1.891	2.273	15

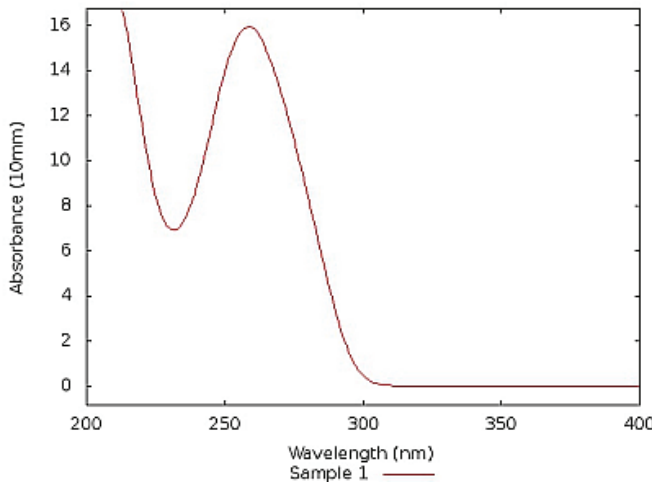


Figure 1: Example outputs of DNA and RNA quantification using Implen Nanophotometers®

# Application Showcase

## Methods

Four datasets of patient populations were used in this study - NACBC Sequencing Set, Internal NACBC Validation Set, External GEO Validation Set (GSE25066) and External TCGA Validation Set, each of varying characteristics.

DNA was extracted from fresh frozen tissue samples and blood samples using the QIAamp DNA Mini Kit and QIAamp DNA Blood Mini Kit (Qiagen). RNA was extracted using TRIzol reagents (Tiangen).

## Nucleic acid quantification

Purity Assessment: The purity of isolated DNA and RNA samples was evaluated using the NanoPhotometer®. The absorbance ratio of 260 nm to 280 nm (A<sub>260</sub>/A<sub>280</sub>) was determined. A ratio within the range of 1.8 to 2.0 indicated pure samples suitable for subsequent experiments.

Concentration Measurement: The concentration of nucleic acids was quantified based on the absorbance at 260 nm. A mass  $\geq 3 \mu\text{g}$  was considered sufficient for sequencing sample library construction.

## Conclusion

Key findings of this study indicate neoadjuvant chemotherapy significantly alters mutation rates, DNA repair pathways, and immune microenvironment. Specifically, the CDKAL1P409L mutation was identified as reducing chemotherapy sensitivity, while amplifications in ADGRA2 or ADRB3 were linked with worse prognosis and treatment outcomes.

The application note highlights the use of Implen Nanophotometer for DNA and RNA quantification. Specifically, after isolating total DNA from fresh frozen tissue samples and blood samples, and extracting RNA from fresh frozen tumour tissue, the purity of the total DNA and RNA was estimated using the NanoPhotometer.

Sample outputs of DNA and RNA quantification using the Implen NanoPhotometer is shown in Figure 1.

## Reference

- Yin, G.; Liu, L.; Yu, T.; Yu, L.; Feng, M.; Zhou, C.; Wang, X.; Teng, G.; Ma, Z.; Zhou, W.; Ye, C.; Zhang, J.; Ji, C.; Zhao, L.; Zhou, P.; Guo, Y.; Meng, X.; Fu, Q.; Zhang, Q.; Li, L. Genomic and Transcriptomic Analysis of Breast Cancer Identifies Novel Signatures Associated with Response to Neoadjuvant Chemotherapy. *Genome medicine* 2024, 16 (1). DOI: 10.1186/s13073-024-01286-8.



Maintenance Free



Full Scan

Implen

NanoPhotometer®  
NP80



Rapid Analysis



## A comprehensive benchtop solution

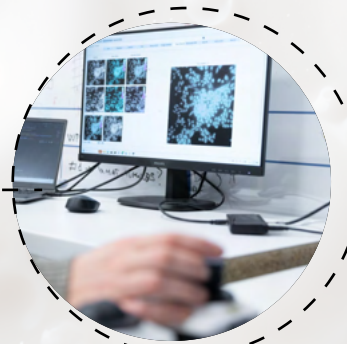


**VioleT 3.0**

Simplifying  
**Fluorescence Lifetime Imaging Microscopy (FLIM) &  
 Förster Resonance Energy Transfer (FRET)**

An all-in-one microscopy platform for **QF-Pro® technology**

High-end modulated laser  
 Sensitive image sensor  
 A multi-channel LED for immunofluorescence.



## Quantifying Functions in Proteins- QF-Pro® Technology

**The New Spatial Biology Standard**

Complemented with our QF-Pro® imaging software and reagent kits  
 Check out few of the available biomarkers-

### Protein – Protein Interaction states:

- PD-1/PD-L1
- CTLA-4/CD80
- TIGIT/CD155
- LAG3/MHCII
- HER2/HER3
- PKB/PDK1

### Post – translational modification:

- PKB phosphorylation (pT308)
- STAT3 phosphorylation (pS727 or pY705)
- PD-1 phosphorylation state (pY248)

# Application Showcase



## Fighting viruses on the nanoscale with AFM

**Understanding structure, function and host interaction of viruses in WaveMode, an off-resonance imaging technique**

**D**uring the last century humans have endured multiple severe viral outbreaks including the Spanish flu and other influenza epidemics, HIV, SARS-CoV, MERS, Ebola and the recent SARS-CoV2 pandemic. During this period, science has made strides in understanding many different facets of virus outbreaks including viral infectivity, pathogenicity, and virulence, transmission, and propensity to cause an epidemic/pandemic. Modern techniques that include cell culture, infectivity assays, polymerase chain reactions, fluorescence microscopy, electron microscopy, and immunoassays have helped us gain a better understanding about the virus life cycle, viral replication, and the virus-host interaction. We now have a better grasp on the structure and function of the viral particle, viral genome, RNA or DNA expression levels, virus-host cell interaction and immune response. These advances have resulted in the development of vaccines and drugs to treat several different viruses.

**Keywords-** Atomic Force Microscopy, AFM, HSV-1 capsids, WaveMode, off-resonance imaging, Nanosurf Drive AFM

### Introduction

Atomic force microscopy (AFM) is one of the newer techniques available for virus research. AFM is a cantilever-based technique that utilizes a sharp tip to interrogate surfaces at resolutions well below the optical diffraction limit. Beyond imaging, AFM is also a powerful tool for nano-mechanical probing and nano-manipulation. AFM thus offers a large toolbox of applications to address structure, function, and host interaction of viruses.

One of the primary advantages of AFM compared to electron microscopy is that it can operate on samples immersed in liquid. This empowers experiments on

# Application Showcase

living cells or cell organelles at physiologically relevant conditions. AFM imaging has been used to study functional/infective virus particles, to investigate the dimension and morphology and packaging of viral genomic material. Beyond imaging, AFM has been used for manipulation of single viruses by force spectroscopy to study early events of virus-host interactions.

This article reports on high-resolution imaging and force spectroscopy on virus capsids attached to both glass substrates and isolated cell nuclei. In this study, virus particles were deposited on a single cell using a hollow cantilever and the host cell response upon virus infection was studied.

## High-resolution imaging and force spectroscopy of Herpes simplex virus 1 capsids

The capability of AFM to observe samples in aqueous environments allows observing proteins, nucleic acids and assemblies thereof in a state that is as close to physiological as possible. Namely, keeping samples such as Herpes simplex virus 1 (HSV-1) capsids fully hydrated allows observing their unperturbed structure as well as investigating their nanomechanics.

WaveMode imaging, a photothermally driven off-resonance operation mode has been utilised to visualize HSV-1 capsids. Adsorption of the HSV-1 capsids to a modified glass surface resulted in weakly attached capsids as the surface area of the capsids interacting with the substrate is rather small due to their shape. As a result, imaging requires gentle conditions not to displace the capsids during the imaging process. WaveMode with its gentle imaging conditions that result in minimal vertical and lateral forces acting on the capsids during imaging allowed reproducible and fast visualization of HSV-1 capsids.

WaveMode imaging reveals fundamental structural features of HSV-1 capsids, such as their size or geometry. Figure 1A shows AFM images of two HSV-1 capsids revealing their icosahedral overall structure and

the arrangement of capsomeres within the different facets of the icosahedral structure.

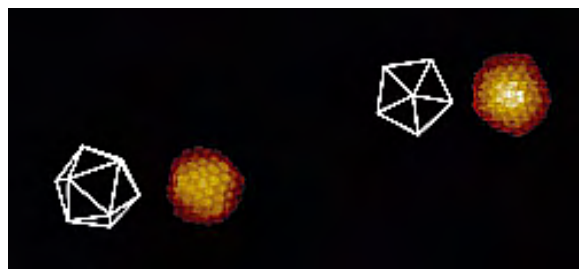


Figure 1A: AFM topography of two virus capsids adsorbed to a modified glass surface. The capsids adsorbed in different orientations. The white wireframes indicate the surfaces of the capsids facing upwards. Image width 940 nm, colour scale 55 nm.

The high resolution of the AFM also allows precisely measuring the diameter of such virus particles. For HSV-1, the measured height depends, because of the icosahedral structure, to some extent on the orientation in which the particles adsorbed to the surface. The examples in Figure 1B show a height of 115 nm.

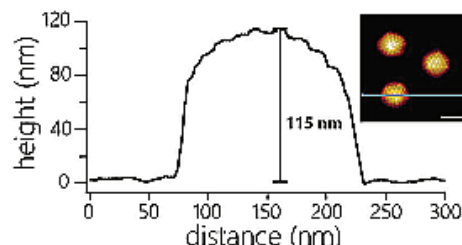


Figure 1B: Cross-sectional profile of one of the three capsids shown in the inset (scale bar 100 nm). The capsid shows an apparent height of 115 nm.

At slightly higher resolution, more details of the capsid structure can be resolved; for example, the center-to-center spacing of capsomeres can be determined (~17 nm; Figure 1C).

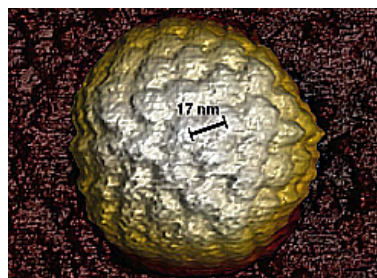


Figure 1C: 3D render of AFM topography of a virus particle at higher resolution than in figure 1A. The individual capsomeres can be observed and the center-to-center distance determined (17 nm).

# Application Showcase

After locating virus capsids with WaveMode imaging, individual capsids can be probed with the AFM probe to obtain the nanomechanical properties of these capsids. It is known, that the nanomechanical properties of virus capsids depend not only on the structure of the protein-based capsid but e.g. also on whether the capsids are filled with DNA or not<sup>1</sup>.

To measure the nanomechanical properties of capsids, the cantilever is approached to the top of the capsid to apply an increasing force to the capsid. Such experiments result force-distance curves such as shown in Figure 2A. The force curves reveal a plethora of information, not only on the nanomechanics of the probed capsid. After contacting the capsid (Figure 2A, left dashed line) and upon application of force, the capsid deforms mainly elastically, as the force-distance curve shows a linear increase. The slope of the force distance curve (Figure 2A, orange line) reveals the spring constant of the capsid.

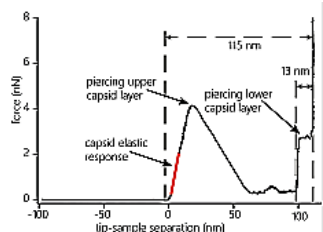


Figure 2A: Indentation curve on an HSV-1 capsid. The curve shows the elastic response (stiffness, orange line) of the capsid upon application of force, the penetration of the upper protein layer and the penetration of the lower capsid layer. The distinct features of the force curve also allow estimating the height of the capsid (115 nm) and the thickness of the protein layer (13 nm).



Figure 2B: 3D render of two capsids after indentation. The capsids were indented with the cantilever until both capsid layers were penetrated and re-imaged. The defect caused by indentation as well as capsomers not directly affected by the indentation can be clearly resolved. Image width: 705 nm.

As the force applied to the capsid increases, the capsid structure at some point fails and cannot withstand the

applied force anymore. The failure point is characterized by a sudden decrease of the force in the force-distance curve. The capsid structure failure occurs locally rather than causing complete capsid destruction: Re-imaging the capsid after penetration reveals a defect at the location where the cantilever interacted with the capsid (Figure 2B).

The force-distance curve also reveals information about the size of the capsid and the thickness of the capsid's protein shell. After piercing the first layer of proteins of the capsid, the tip is further approached towards the surface and at some point, meets the inside of the shell at the bottom of the capsid (Figure 2A, middle dashed line) and further movement loads the lower protein layer of the capsid from the inside. At sufficient force, also this protein layer is pierced and the tip pushes through and subsequently interacts with the underlying glass substrate (Figures 2A, right dashed line). The distance between the initial contact point with the capsid and the position at which the tip interacts with the glass surface reveals the capsid height at the point of indentation (~115 nm). The distance between contacting the lower protein layer and the interaction with the glass surface reveals the thickness of the capsid shell (~13 nm).

## Imaging of HSV-1 capsids bound to isolated cell nuclei

In vivo, after entry into the cell HSV-1 capsids dock to nuclear pore complexes (NPCs) on the outer surface of the cell nucleus to release their DNA into the cell nucleus. Evilevitch and Tsimtsirakis established a reconstituted virus-nucleus system that allows investigating the nanomechanical changes taking place upon DNA injection and reorganization of chromatin inside the nucleus<sup>2</sup>.

WaveMode revealed for the first time high-resolution topographic information of HSV-1 capsids on intact nuclei and not just spread, flat nuclear membranes. The AFM images reveal individual HSV-1 capsids bound to NPCs as well as NPCs not occupied by capsids. (Figure 3A). With WaveMode imaging, capsids bound to the soft

# Application Showcase

nuclei can be readily recognized by the individual capsomeres that can be observed. (Figure 3B).

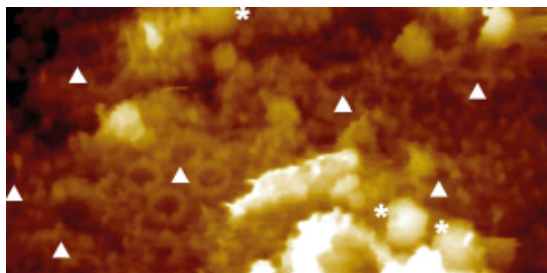


Figure 3A: Overview image of the surface of an intact isolated and fixed nucleus. The image reveals NPCs ( ) and HSV-1 capsids (\*) bound to NPCs. Image width 1650 nm.

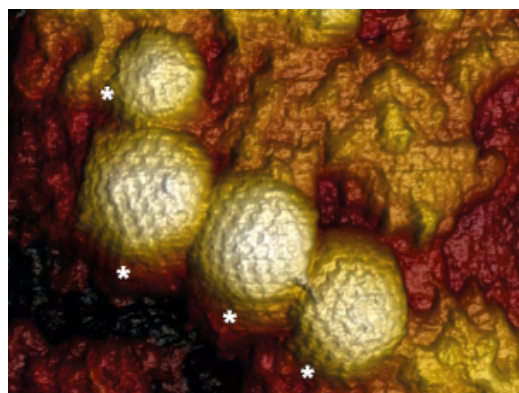


Figure 3B: 3D rendered AFM topography of multiple HSV-1 capsids bound to an intact nucleus. Image width 590 nm.

The reconstituted virus-nucleus system not only allows imaging NPC-bound HSV-1 capsids but also determining nanomechanical properties of nuclei under different conditions. Figure 4A shows a representative indentation curve on a nucleus incubated with DNA-containing HSV-1 capsids. Repeated indentation of multiple capsids reveals a Young's modulus of  $214 \pm 10$  kPa (average  $\pm$  SE) for nuclei incubated with C-capsids (Figure 4B).

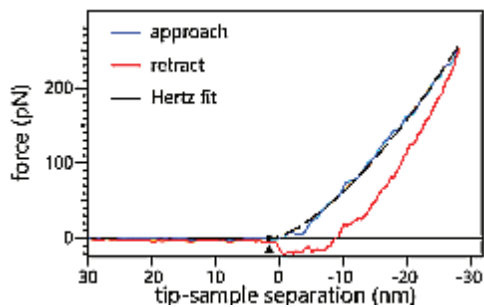


Figure 4A: Representative indentation curve on a non-fixed nucleus incubated with C-capsids. The dashed line represents the fit of the Hertz model to the data.

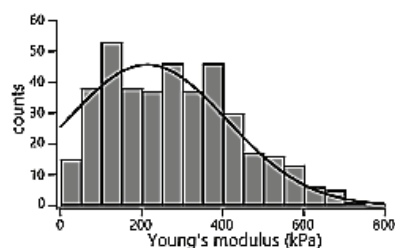


Figure 4B: Histogram of Young's moduli from repeated probing of multiple non-fixed intact nuclei incubated with C-capsids.

## Conclusion

Virus research in the past has led to the development of treatments and vaccines. New viruses like the recent SARS-CoV2, which has led to the COVID-19 pandemic, stressing the importance of continued virus research to become a better and faster response to future outbreaks. AFM is a powerful technique to analyse structure and nanomechanics and manipulate biological samples under physiological conditions. It can be combined with advanced optical techniques, to allow correlation of optical characterization of the sample cells in parallel to the AFM experiments.

This application successfully explores the structure and nanomechanics of virus capsids using the WaveMode, an off-resonance imaging mode by Nanosurf Drive AFM.

## References

1. Martín-González, N.; Hernando-Pérez, M.; Condezo, G. N.; Pérez-Illana, M.; Šiber, A.; Reguera, D.; Ostapchuk, P.; Hearing, P.; San Martín, C.; de Pablo, P. J. Adenovirus Major Core Protein Condenses DNA in Clusters and Bundles, Modulating Genome Release and Capsid Internal Pressure. *Nucleic Acids Research* 2019, 47 (17), 9231–9242. DOI: 10.1093/nar/gkz687.
2. Evilevitch, A.; Tsitsirisakis, E. Reconstituted Virus–Nucleus System Reveals Mechanics of Herpesvirus Genome Uncoating. *QRB Discovery* 2021, 3. DOI: 10.1017/qrd.2021.14.



**DriveAFM**

# Application Showcase

**PRECISION**  
X-RAY IRRADIATION

## Efficient siRNA delivery to TNBC cells using polymer - lipid nanocomplexes

### Exploring the role of Precision X-Ray Imaging in cancer biology

DNA double – strand breaks (DSBs) are a primary mechanism that causes cancer cell death. DSBs are a result of radiation therapy given to combat cancer. This resulting damage to the DNA can however trigger a cascade of activations of DNA repair mechanism, lessening the impact of radiation therapy.

This article highlights the use of Precision X-ray's imaging systems in the delivery of siRNA through novel polymer - lipid based nanocarrier.

Keywords: DNA damage, radiotherapy, Precision X-Ray, breast cancer, siRNA

### Introduction

One of the therapeutic approaches for combating breast cancer is radiation therapy. It triggers various forms of DNA damage via the use of ionising radiation. Destruction of DNA is accompanied by DNA double-stranded breaks (DSBs), proven to be most harmful in causing cancer cell death.

While radiation therapy is successful in delivering the intended DNA damage, its perverse effect is activation of DNA repair mechanisms. Cancer cells often develop resistance to this treatment by activating their DNA damage response (DDR) machinery, which repairs DSBs. RAD50, a SMC protein (Structural Maintenance of Chromosomes) along with heterotrimeric recombination 11 homolog 1 (Mre11) and Nijmegen breakage syndrome protein 1 (NBS1) form the MRN complex, which binds to damaged and broken DNA to exhibit various enzymatic activities that are crucial for the repair of DSBs.

# Application Showcase

Silencing RAD50 in cancer cells using small interfering RNA (siRNA) to enhance breast cancer chemotherapy has been explored. However, delivering siRNA to target cells and their cytoplasm poses significant obstacles, including degradation by RNAases, accumulation and penetration within tumours, cellular uptake, and entrapment and degradation within endosomes/lysosomes. To overcome these challenges, various nanocarrier systems have been developed to improve siRNA *in vivo* stability, tissue bioavailability, and transfection efficiency.

To help achieve the development of novel polymer-lipid based RAD50 siRNA loaded nanoparticles, Precision X-Ray systems have been employed, as highlighted in this application note.

## Experimental

MDA-MB-231 cells, a triple-negative breast cancer (TNBC) cell line, and MCF-10A cells, a non-malignant

breast cell line, were acquired and cultured in Dulbecco's Modified Eagle's Medium (DMEM).

The RAD50-siRNA-NPs were prepared in an oil - water emulsion. This was followed by assessment of siRNA encapsulation, *in vitro* transfection of RAD50 siRNA into cells and investigation of internalization and intracellular localization of siRNA-NPs.

To assess the effect of RAD50-siRNA-NPs treatment and RT on DNA damage repair, MDA-MB-231 cells were treated with RAD50-siRNA-NPs or free-siRNA and then irradiated with a single dose of 5 Gy using X-RAD 320 system (Precision X-Ray, Madison, CT, USA; 320 kV, 2.7 Gy/ miFor evaluation of *in vivo* RAD50 silencing and biomarkers, the tumours were exposed to radiation (10 Gy) using small animal irradiator (SmART+) XRAD system (Precision X-Ray Inc., Madison, CT, USA).

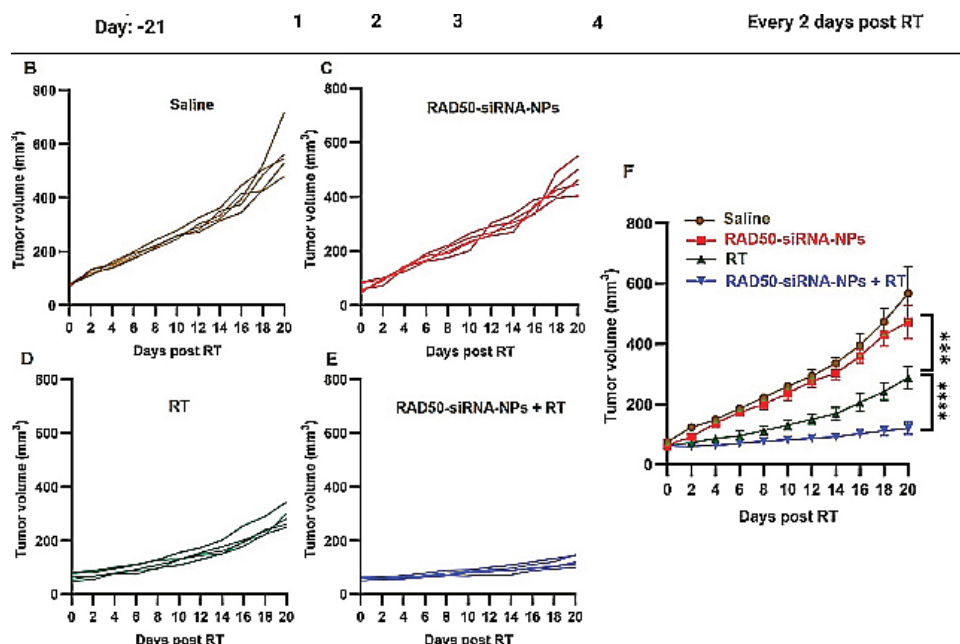


Figure 1: RAD50 silencing by RAD50-siRNA-NPs plus RT inhibited tumor growth of MDA-MB-231 tumor-bearing mice. (A) Schematic of treatments of RAD50-siRNA-NPs and RT of orthotopic MDA-MB-231 tumors grown in SCID mice. (B) Individual mouse tumor growth curves for saline group, (C) RAD50-siRNA-NPs group, (D) saline + RT (10 Gy) and (E) RAD50-siRNA-NPs + RT treated animals. (F) Comparison of tumor growth curves for the four treatment groups, saline, RAD50-siRNA-NPs (0.5 nmol siRNA), saline + RT alone (10 Gy), and RAD50-siRNA-NPs (0.5 nmol siRNA) + RT (10 Gy) treatment, 5 mice in each group.

# Application Showcase

## Conclusion

This application highlights the use of Precision X-Ray imaging systems. The X-RAD 320 was critical in applying radiation therapy (RT) on the MDA-MB-231 cells that rendered a controlled assessment of the fate of DNA damage repair after treatment with RAD50-siRNA-NPs. Furthermore, the SmART+ XRAD system provided in vivo radiation with precision such that RAD50 silencing, and its biomarkers could be evaluated in tumour models. These results emphasize the role of Precision X-Ray imaging systems in improving our comprehension of cancer and leading to new treatments of it.

The results showed that the nanoparticles successfully delivered siRNA into the cells, silenced RAD50 expression, and increased radiation-induced DNA damage. suggesting that targeting RAD50 with siRNA-NPs could be a promising strategy to improve radiation therapy outcomes for breast cancer.

## References

1. Zetrini, A. E.; Abbasi, A. Z.; He, C.; HoYin Lip; Ibrahim Alradwan; Rauth, A. M.; Henderson, J. T.; Xiao Yu Wu. Targeting DNA Damage Repair Mechanism by Using RAD50-Silencing SiRNA Nanoparticles to Enhance Radiotherapy in Triple Negative Breast Cancer. *Materials Today Bio* 2024, 28, 101206–101206. DOI: 10.1016/j.mtbiol.2024.101206.



**Image SmART, Plan SmART,  
Treat SmART**



## Features

- Compact, user-friendly design
- Level detection system prevents bottle overfill
- Control knob for vacuum setting
- The parts in contact with liquids are autoclavable
- Easy to disassemble and clean
- Ideal tool to avoid lab air contamination and protect personnel safety
- Adjustable vacuum level with indicator light is designed for various applications

**inkarp®**  
Your Knowledge... Our Solution...!

Authorised India Partner

## Applications

For laboratory waste recovery and separation of liquid and solid.

It can be widely used in cell culture, DNA extraction, microplate waste removal, and any other liquid separation or recovery.

Integrating SafeVac with a biosafety cabinet enhances waste management, increases safety, and improves operational efficiency in laboratories dealing with hazardous materials.



Pair it with your biosafety cabinet!

# SafeVac

## Vacuum-Controlled Aspiration System

Safe and efficient system for labs handling critical or biological liquid waste.

**DVAB**

**PMEC**  
India

26-27-28 November 2024, Delhi  
Stall No: RH.C62, Hall No: Hall A

OCTOBER 2024  
info@inkarp.co.in

# Application Showcase



## Native and staining-free pharmacologic assessment of drug dose responses

### Holographic analysis of single cells using anvajo fluidlab R-300 - Cell Counter & Spectrometer

**C**ell viability assays are crucial for understanding the pathways involved in cell survival or death post exposure to toxic agents. These assays are generally used in drug screening and biomedical applications. Conventionally, these methods rely on laborious staining procedures and the use of cytotoxic reagents, often limiting their speed and accuracy. This comparative study emphasizes on the advantages of fluidlab R-300 as a rapid and reliable label-free method for assessment of cell viability compared to established colourimetric assays.

**Keywords:** Cell viability, staining, fluidlab R-300, colourimetric, assay, MTT, resazurin

### Introduction

A sensitive and reproducible cell viability assay is essential for monitoring cell health in cell culture laboratories. Moreover, viability assays are a fundamental tool in the drug discovery process as well as in the assessment of cytotoxicity. Assaying cell viability typically involves biochemical methods, such as dye exclusion stains to probe membrane intactness, DNA intercalating agents or metabolic assays that emit fluorescence based on enzymatic activity.<sup>1,2</sup> However, this involves additional incubation and handling steps of mostly cytotoxic reagents leading to additional error sources, and prolonged experimental time.

In contrast, the fluidlab R-300 detects viability based on morphological and foremost compositional changes occurring during cell death. The change in composition e.g. reflects protein turn-over and can be assessed due to the quantitative nature of the phase signal in the fluidlab R-300's innovative holographic microscope.

# Application Showcase

This technological novelty makes additional handling and staining steps unnecessary, and the percentage of viable cells is directly accessible from a cell suspension.

In this proof-of-concept study, we compared the performance of the label-free viability tool of the fluidlab R-300 to two well-established colourimetric viability readouts. Colourimetric viability assays use a variety of markers as indicators of metabolically active (living) cells. The cell-permeable reagents are reduced by metabolically active cells to strongly coloured reporter molecules, whose fluorescent signal is proportional to the number of living cells in the sample. These colourimetric assays are commonly used as a screening method to determine the cytotoxic potential of drugs. We show that the staining-free viability tool of the fluidlab R-300 can be reliably used for monitoring cell health and for assessing dose response curves in pharmacology.

## Methods

### Cell culture & preparation

Cells were plated at a density of 1500 cells per well in triplicate in 96-well plates. Cells were allowed to attach and grow at 37 °C, 5% CO<sub>2</sub> for 24 h. Subsequently, the small molecule drugs staurosporine or GI254023X were added to cells in triplicate wells, at concentrations ranging from 0.1 nM to 1000 nM (for staurosporine) or 1 µM to 1000 µM (for GI254023X). Cells were treated for 4 days at 37 °C, 5% CO<sub>2</sub>.

Cell lines used	
U87MG	Cancer cells
MCR5	Fibroblasts
HL-1	Cardiomyocytes

### Cell viability assays

To assess cell viability, two colourimetric assays (MTT and resazurin based assays) were compared to the staining-free viability tool of the fluidlab R-300. For the colourimetric cytotoxicity assays, medium was replaced

concentration 0.015 mg/ml) was directly added to 200 µl culture medium per well. After incubation with the dye for 4 hours, absorbance was read out at 570 nm with a BioTek Synergy HTX Multi-Mode microplate reader.

For the staining-free viability assay, cells were detached from the wells by adding 30 µl of trypsin for 4 min. The trypsin reaction was stopped by adding 30 µl of culture medium. For each replicate, 20 µl of cell suspension was loaded into the acella100 sample carrier and viability was assessed using the fluidlab R-300. For all three assays, cell viability was normalized to the viability of the untreated DMSO control sample.

Material Reagents	Reagents
fluidlab R-300	cell culture medium
acella100 sample carrier	thiazolyl blue tetrazolium bromide (MTT)
microplate reader	resazurin cell viability kit
96-well plates	staurosporine, GI254023X
	trypsin

## Results

Cell death was induced by treating three different cell lines with small molecule drugs that cause cell death through apoptosis. Triggering of apoptosis causes specific molecular changes together with morphological changes, such as cell shrinkage, membrane fragmentation and nuclear condensation. These changes in protein content and cell morphology can be visualized by the state-of-the-art digital holographic microscopy method used in the fluidlab R-300. Every cell in the sample is analysed by convolutional neural networks to determine whether it is dead or alive. Live cells are characterized by a dark contour and a structured cytoplasm, while dead cells lose their well-defined boundary and appear black. Figure 1 (A – F) shows exemplary cell images obtained with the fluidlab R – 300.

# Application Showcase

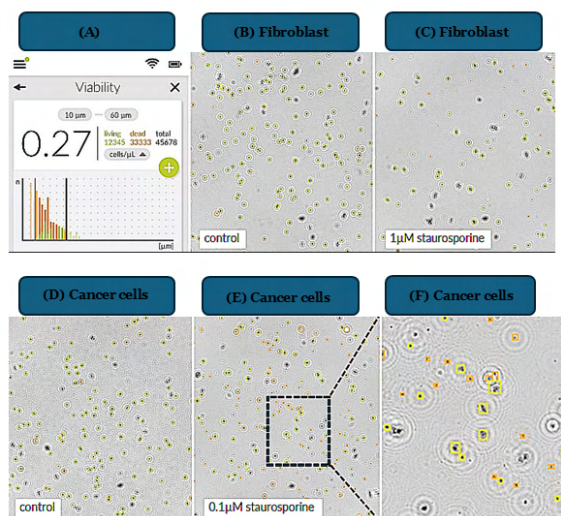


Figure 1: Staining-free viability measurements with the fluidlab R-300. (A) Result screen of the fluidlab R-300 showing the percentage of viable cells and the total cell count for dead and alive cells. Representative images of (B) control fibroblasts (MCR5) cells, (C) fibroblast cells treated with 1  $\mu\text{M}$  staurosporine, (D) control cancer cells (U87MG) and (E) cancer cells treated with 0.1  $\mu\text{M}$  staurosporine. Live and dead cells are marked with green and orange boxes, respectively. (F) Zoom in on the region labelled with the blue rectangle in (E) to show the distinct morphology of dead and alive cells.

Cell viability was measured using the staining-free viability tool of the fluidlab R-300 and two colourimetric assays (MTT and resazurin viability assay). The percentage of viable cells in the sample was monitored at different drug concentrations. Treatment of all three cell lines with staurosporine—a general protein kinase inhibitor and potential anti-cancer therapeutic—showed a concentration-dependent decrease in the percentage of living cells. Additionally, cancer cells (U87MG) were treated with GI254023X, a metalloproteinase inhibitor inducing apoptosis. All three viability assays show comparable dose – response curves for the three different cell lines tested. By fitting the dose – response curves with a sigmoidal function, the half-maximal inhibitory concentration ( $\text{IC}_{50}$ ) for each assay was determined. According to the  $\text{IC}_{50}$  values, cardiomyocytes (HL-1) were more sensitive to staurosporine than cancer cells (U87MG) and fibroblasts (MCR5). The staining-free viability tool of the fluidlab R-300 proved to perform similarly as the colourimetric assays (Figure 2A–2D).

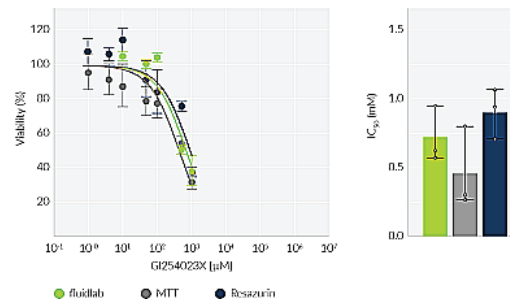


Figure 2A: Cancer Cells U87MG

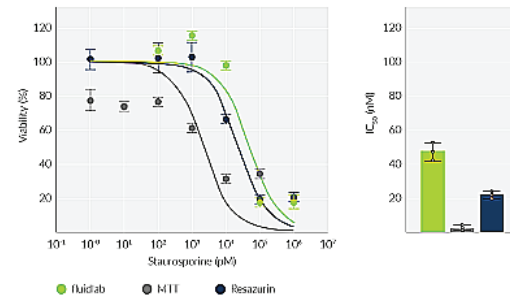


Figure 2B: Fibroblasts MCR5

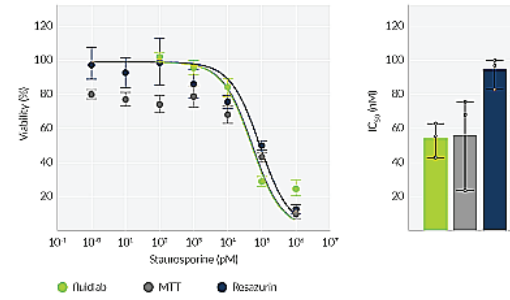


Figure 2C: Cancer Cells U87MG

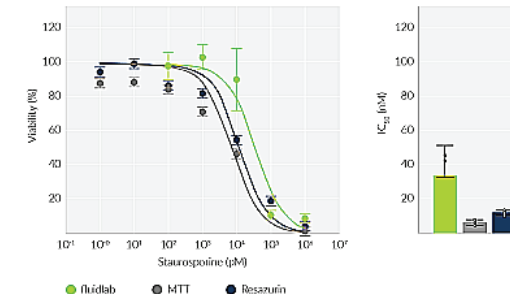


Figure 2D: Cardiomyocytes – HL-1

Figure 2(A–D): Comparison of different cell viability assays for drug screening. Dose-response curves were measured for two different drugs (staurosporine and GI254023X) for three different cell types. The percentage of viable cells and  $\text{IC}_{50}$  values were determined using the fluidlab R-300 (green), the MTT assay (grey) and the resazurin assay (blue). Averages and standard errors of the mean were derived from triplicates.

# Application Showcase

Assay	Staurosporine IC <sub>50</sub> (nM)		
	Cancer cells	U87MG Fibroblasts	MCR5 Cardiomyocytes HL-1
fluidlab R-300	54 ± 10	48 ± 5	34 ± 17
MTT assay	56 ± 29	2.2 ± 0.4	7 ± 2
resazurin assay	94 ± 7	23 ± 2	12 ± 1

## Conclusion

Here, we showed that the staining-free viability tool of the fluidlab R-300 can be successfully employed for monitoring cell viability in the cell culture environment. The label-free analysis of the fluidlab R-300 was developed to work across a large range of cell types. Here, we showed that the fluidlab R-300 reliably detects cell viability for three different cell types with distinct morphology. We compared its performance to two colourimetric assays based on quantification of metabolic activity that are commonly used techniques in the drug screening process. While all three assays yield comparable results, the fluidlab R-300 offers the distinct advantage of assessing cell viability without introducing fluorescent dyes into the culture. In contrast, the MTT and resazurin viability assays require pre-analytical staining and incubation steps, which are not just more time-consuming, but may also introduce artefacts due to staining. Long exposure of cells to dyes can induce cytotoxicity and thereby the assay itself may bias the quantification of the percentage of viable cells in a cell culture sample.<sup>1,2</sup> Moreover, a variety of chemical compounds have been shown to interfere with MTT and resazurin reagents leading to significant conversion of the assay reagents even in the absence of any cellular activity.<sup>3</sup>

In summary, the automated imaging and quantitative analysis approach of the fluidlab R-300 allows for the testing of cytotoxic compounds and is suited for the assessment of cell viability in numerous biological assays without the need for additional staining.

## References

- Riss, T. L.; Moravec, R. A.; Niles, A. L.; Duellman, S.; Benink, H. A.; Worzella, T. J.; Minor, L. Cell Viability Assays. Nih.gov. <https://www.ncbi.nlm.nih.gov/books/NBK144065/>.
- Aslantürk, Ö. S. In Vitro Cytotoxicity and Cell Viability Assays: Principles, Advantages, and Disadvantages; IntechOpen, 2017.
- Neufeld, B. H.; Tapia, J. B.; Lutzke, A.; Reynolds, M. M. Small Molecule Interferences in Resazurin and MTT-Based Metabolic Assays in the Absence of Cells. Analytical Chemistry 2018, 90 (11), 6867–6876. DOI: 10.1021/acs.analchem.8b01043.



## fluidlab R-300

### Cell Counter & Spectrometer

# Application Showcase



## Exploring cell-based liquid biopsy: beyond circulating tumour cell enumeration

### Utilising RareCyte platform for comprehensive protein biomarker and cancer genomics analysis

Liquid biopsy—the sampling of blood—is a non-invasive method for generating information previously only available from tissue biopsies of the tumour mass. However, it cannot assess cancer phenotypes, including the expression of drug targets and protein biomarkers. Circulating tumour cells (CTCs) are intact cancer cells that have entered the blood that have the potential for distant metastasis. While enumeration of CTCs is prognostic of outcome, recently developed technology allows for the interrogation of protein biomarkers on CTCs that could be predictive of response. Together ctDNA and CTC analysis can enhance the capabilities of liquid biopsy in modern medicine.

**Keywords:** Liquid biopsy, circulating tumour cell, CTC, protein biomarker, single cell sequencing, drug target, companion diagnostics, RareCyte

### Introduction

Liquid biopsy, a non-invasive method, analyses of blood samples for circulating tumour DNA (ctDNA) and circulating tumour cells (CTC). There are many advantages of liquid biopsy testing, including ease of access to samples, minimal procedural discomfort and complications, integration of tumour information from various locations throughout the body, real-time data rather than historical snapshot, and longitudinal sampling.

CTCs are intact cancer cells that have left the tissue compartment to enter the vascular compartment. There are two critical points regarding CTCs that are fundamental to the pathophysiology of tumour metastasis and progression, yet these are not widely recognized. The first is that each distant tumour metastasis was once a CTC. The second point is that viable CTCs that are present during cancer therapy are resistant to treatment.

# Application Showcase

CTCs therefore represent a population of cells that can be investigated for mechanisms of resistance even if the therapy is successful in reducing tumour burden. These mechanisms may be phenotypic as well as genotypic. CTC liquid biopsy thus collects tumour cells with both metastatic and resistance potential.

## The RareCyte Liquid Biopsy Platform

The CTC analysis workflow includes four steps: sample processing (AccuCyte system—blood collection, nucleated cell density separation, and slide preparation), immunofluorescence staining (RarePlex® kits), imaging (CyteFinder instruments—automated 7-channel scanning microscopes, analysis software) and nucleic acid sequencing (CytePicker® device, located above the stage in the CyteFinder instrument, Figure 1).

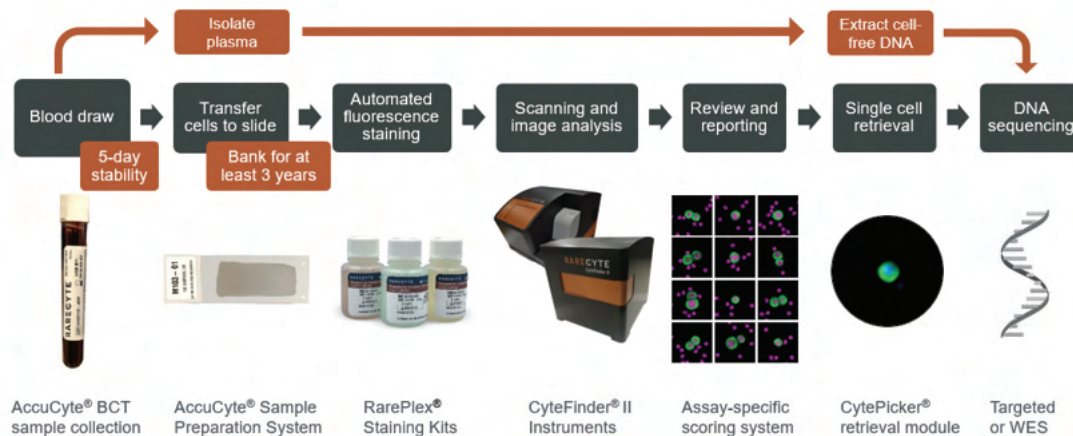


Figure 1: RareCyte liquid biopsy workflow

## Protein Biomarker Applications

### Tumour characterization

RareCyte platform offers additional biomarker channels that enable investigation of markers that may be known to be clinically significant within a tumour type, or of investigational interest.

The RareCyte platform has quantified and analytically validated assays for various markers— androgen receptor (AR), AR splice variant 7, and synaptophysin (prostate cancer), HER2 and ER (breast cancer), and PD-L1 (immune-oncology).

The platform has also qualified additional markers, including PSMA, PSA, Muc1, progesterone receptor, EGFR, HER3 and Ki-67 for various epithelial cancers. These markers can be used in combination to define phenotypic subsets of cells. For instance, breast cancer CTCs can be divided into ER+/HER2+, ER+/HER2-, ER-/HER2+ and ER-/HER2-groups and their presence followed over time.

### Diagnostic confirmation

Liquid biopsy can be used in situations where invasive procedures are not feasible due to risk, cost or lack of access.

The detection of CTCs via a blood sample that includes confirmatory markers of tissue origin (EGFR in lung cancer or HER2 in breast cancer and GI malignancies, for

instance) may establish a non-invasive alternative for cancer diagnosis and treatment.

### Companion diagnostics development

Drug targets and protein markers of therapeutic efficacy can be evaluated on actual tumour cells in the blood using CTC-based liquid biopsy. This provides a rational approach to the development of non-invasive companion diagnostics that are not sequence based.

### Tumour transformation

Lineage differentiation biomarkers track changes in tumour subtypes. Synaptophysin expression on CTCs,

# Application Showcase

can indicate neuroendocrine differentiation, offering a rational minimally invasive alternative to tissue biopsy.

## Pharmacodynamic investigation

It is difficult to study drug – target interactions through sequential tumour biopsies. CTC biomarker assays make possible the assessment of drug activity via downstream markers known to be modulated by drug action.

## Non-epithelial cancers

Most studies of CTCs focus on epithelial tumours. First generation CTC technologies rely on epithelial surface markers to capture CTCs from the blood. However, this limits the detection of non-epithelial cancer CTCs. The RareCyte platform allows flexible substitution of other markers for specific identification of the cell types, such as S-100, melan-A, and NG2 for identification of circulating melanoma cells.

## Nucleic Acid Sequencing Applications

### Targeted mutation analysis

Targeted mutation analysis is effective for ctDNA sequencing but can be limited by allelic fraction and ctDNA amount for confident mutation detection. CTCs contain “pure” cancer genomes, minimizing if not eliminating the influence of allelic fraction on sensitivity. The RareCyte platform has been used to identify actionable PIK3CA mutations in CTCs that were not identified in plasma using the same targeted panel in patients with metastatic breast cancer.

### Whole genome/exome sequencing

CTCs contain the entire intact cancer genome, allowing genome wide sequencing that can be employed for broad detection of mutations. The RareCyte platform has been used together with whole exome sequencing to follow the genomic evolution of CTCs in triple-negative breast cancer over the course of 9 months.

### Breakthrough/resistant clone detection

Apoptotic cells are understood to release ctDNA fragments detectable in plasma, but resistant clones are less likely to undergo apoptosis, so their genomes may

not be detected at the current limit of sensitivity of cell-free DNA assays.

There is a rational basis for higher representation of resistant clones within the viable CTC population. Isolating and sequencing CTCs during therapy can identify actionable mutations within the resistant population for targeted treatment planning.

## Tumour cell heterogeneity

ctDNA analysis can assess mutational heterogeneity within a tumour population but cannot analyse individual cells. CTCs, which can be sequenced individually, can better reflect clonal variability and resistance mechanisms, providing a more accurate understanding of heterogeneity at the cellular level.

## Clinical Examples

### CTC enumeration and biomarker analysis

In a clinical study of patients with advanced gastrointestinal cancers, CTCs were counted and followed during treatment.

Figure 1A shows rapid drops in CTC counts in responding patients. Using two dual-biomarker assays (EGFR/Ki-67 and HER2/PD-L1), four biomarkers were investigated.

Figure 1B shows a cluster of CTCs positive for EGFR and Ki-67, and a single CTC positive for HER2 and PD-L1 from a patient with esophageal cancer.

### Targeted panel sequencing of individual CTCs

CTCs from a colorectal cancer patient were retrieved from slides after imaging for hotspot sequencing. The presence of an APC nonsense mutation was detected in three of eight CTCs. This is described in detail in Figure 2.

# Application Showcase

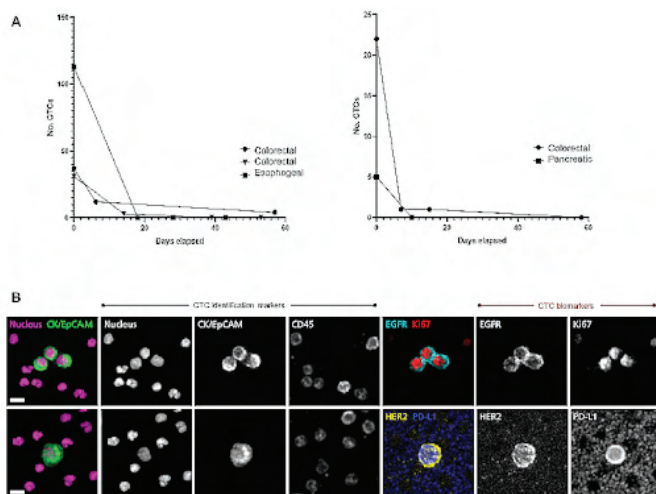


Figure 1: Longitudinal monitoring of CTC counts and characterization of CTC biomarkers. The RareCyte platform was used to study CTCs in a diverse set of gastro-intestinal cancer patients with advanced disease (A) Decreased in several patients with various cancer types following treatment. (B) CTC characterisation using dual - biomarker assays to assess EGFR, Ki-67, HER2 and PD-L1. CTCs from a patient with progressing esophageal cancer showed proliferation (EGFR, Ki-67) and immune checkpoint marker expression (HER2, PD-L1).

Sample	Image of picked CTC	APC R283*	Variant allele frequency	CTCs	WBCs	Calculated % cancer genome
WBC1	N/A	0%	0	4	N/A	
WBC2	N/A	0%	0	5	N/A	
CTC1		0%	1	2	33%	
CTC2		4%	1	5	17%	
CTC3		0%	1	4	20%	
CTC4		0%	1	1	50%	
CTC5		22%	1	3	25%	
CTC6		25%	1	5	17%	
CTC7		37%	1	2	33%	
CTC8		0%	1	3	25%	

Figure 2: Targeted panel sequencing of 8 CTCs from a colorectal patient identified an APC nonsense mutation (R283\*) in 3CTCs. The image of a retrieved CTC is shown, along with co – retrieved WBC and calculated cancer genome fraction.

CTCs were isolated using the RareCyte platform, sequenced using a 65-gene cancer hotspot panel and analysed for somatic mutations.

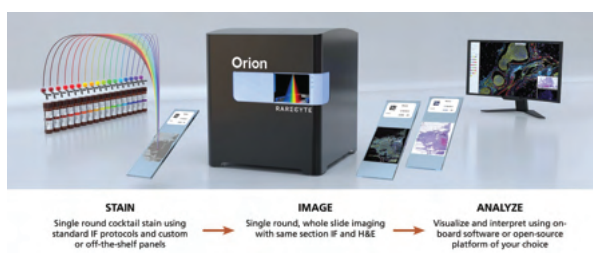
## Conclusion

This application note describes a variety of CTC protein biomarker and sequencing applications in research and diagnostics based on an established liquid biopsy technology platform.

The promise of liquid biopsy is that it will be able to do what tissue biopsy has done—generate essential information for the diagnosis, phenotyping and molecular analysis of cancer. The challenge for liquid biopsy is to combine appropriate technologies with robust assay methods that can extract that information from blood components. ctDNA sequencing has rapidly gained adoption as a mutational testing method. We have described here how the phenotypic and molecular analysis of CTCs can supplement ctDNA sequencing to advance the capacity of liquid biopsy to meet the requirements of twenty-first century medicine.

## Reference

- Kaldjian, E. P.; Ramirez, A. B.; Costandy, L.; Ericson, N. G.; Malkawi, W. I.; George, T. C.; Pashtoon Murtaza Kasi. Beyond Circulating Tumor Cell Enumeration: Cell-Based Liquid Biopsy to Assess Protein Biomarkers and Cancer Genomics Using the RareCyte® Platform. *Frontiers in Pharmacology* 2022, 13. DOI: 10.3389/fphar.2022.835727.



# Inkarp's Proud Moments

Honouring Excellence: Mr. S. Balu, Chairman – Managing Director, Receives Lifetime Achievement Award from the Indian Analytical Instruments Association



 Indian Analytical  
Instruments Association

You know, when I think about how it all started back in 1985 with Inkarp, it was not about big visions or grand plans. It was just a simple idea—to serve people with integrity and offer solutions that made a real difference, while keeping in mind that I had to earn my daily bread. What we had back then was not much, but we had honesty,

and we had our word. That was all that mattered. Over time, this commitment became the bedrock of Inkarp.

In those early days, we worked from my own home. And here, I must give a special thanks to the Inkarp'ians, who accepted the situation with such grace. Imagine starting

work in a house, where you could hear my wife cooking in the kitchen, and the smell of food tempting everyone. I doubt if any employee in any company would agree to such a setup today. But you all stood by me, and that made all the difference. If it were not for that trust, Inkarp would not be where it is today.

Every milestone we have crossed has been because of the people I have worked with. Our customers, who trusted us even when we were just getting started, and our principals, who believed in our ability to represent their brands in India. And of course, the Inkarp'ians. You have all been the driving force behind what we have built together. I am proud that the Lifetime Achievement Award, given to me by Dr. Srivari Chandrasekhar, former Secretary of the Department of Science and Technology, is not just a personal achievement but a recognition of the entire journey we have been on together. Dr. Chandrasekhar, a stalwart in the scientific community and someone who was a customer for me personally decades ago, has seen firsthand how we started from humble beginnings. His presence and acknowledgment at this moment made it all the more meaningful. He is not just a chief guest, but a symbol of the relationships we have nurtured along the way.

Inkarp is not just a company name. It is a reflection of who we are and how we operate. Integrity, Nurture, Knowledge, Accountability, Relationships, and Performance—these are not just words.

They have been our guiding principles from the very beginning. We built this company on the promise of integrity, making sure that every action, every decision, was rooted in honesty.

We nurtured relationships, understanding that growth is not just about us, but about the people we work with—our customers, employees, and partners. Knowledge has always been our compass. Even as a young company, we made the best use of the expertise we had to offer the right solutions. Trust was not easy to come by, but we earned it, one step at a time.

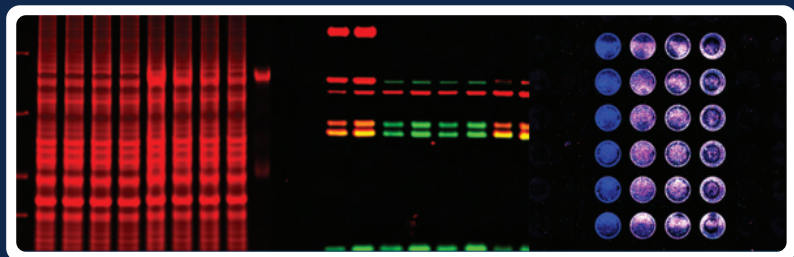
And accountability? From the beginning, we made sure that every promise we made, we delivered on. Our customers and employees knew they could count on us. Relationships have always been at the heart of everything we do. The connections we build today shape the future success we all share.

Performance was never just about doing the job. It was about doing it better, exceeding expectations, and setting a standard for others to follow. This performance-driven mindset is what has shaped Inkarp into what it is today—a place where science thrives, and innovation has no limits. In today's world, the word 'competition' is often misunderstood. People think it is about talking bad about each other's brands. But competition is one of the key reasons for growth. I have always trusted my competitors. In the early stages of Inkarp, I knew none of them would misguide me, and that trust helped us grow. I strongly believe that we should all work alongside the competition, ensuring that no one is "killed" in the market. Instead, we should grow together in this huge industry and encourage more entrepreneurship. This is what will create more employment opportunities and keep the industry thriving. As Ratan Tata once said, "If you want to walk fast, walk alone. But if you want to walk far, walk together."

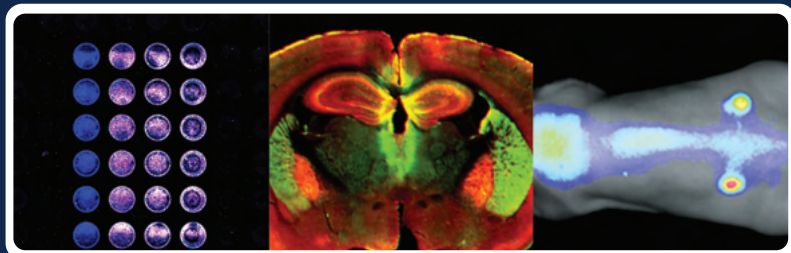
When I look back today, I can see how far we have come, but it is clear that our success is not just ours. It belongs to every customer who believed in us, every principal who trusted us to represent them, and every Inkarp'ian who put in the hard work to make things happen. Our mission has always been to provide solutions that help science progress, and our vision remains simple—continue to be a trusted partner in the journey of discovery and innovation. So, thank you. To our customers, our principals, and especially to the Inkarp family. Together, we have built something special, and together, we will continue to grow, innovate, and make a lasting impact.

**- S. Balu**  
CMD Inkarp Group

# Application Showcase



## Detailed description of Tissue Section Imaging



### Explore a tissue sectioning protocol with LICORbio's Odyssey® Imagers

Tissue section imaging is useful for identifying cellular or tissue localization and expression of biological targets *ex vivo*. Targets can include proteins, DNA/RNA, and labelled small molecules. There are a variety of methods for target detection, including antibody-based detection, visual stains, and labelled probes. With the appropriate equipment, you can assess both the macro- and micro-locations of your target.

This application outlines the protocol for tissue section imaging using LICORbio's Odyssey® Imagers

**Keywords:** Tissue section imaging, IHC, Immunostaining, Odyssey,

### Introduction

#### Overview of Immunohistological Staining

Tissue section imaging is vital to advancing scientific understanding across many disciplines. In clinical and research settings, scientists use tissue sections to diagnose illnesses, to assess therapeutic agent colocalization, to understand diseases, and to characterize treatments.

Figure 1 outlines a general protocol for preparing and staining tissue sections. Details of each step are described in the upcoming sections.

As seen in the workflow, several steps will vary with the requirements of the specific assay. The most conventional protocol for tissue section imaging has been described in this application.

# Application Showcase

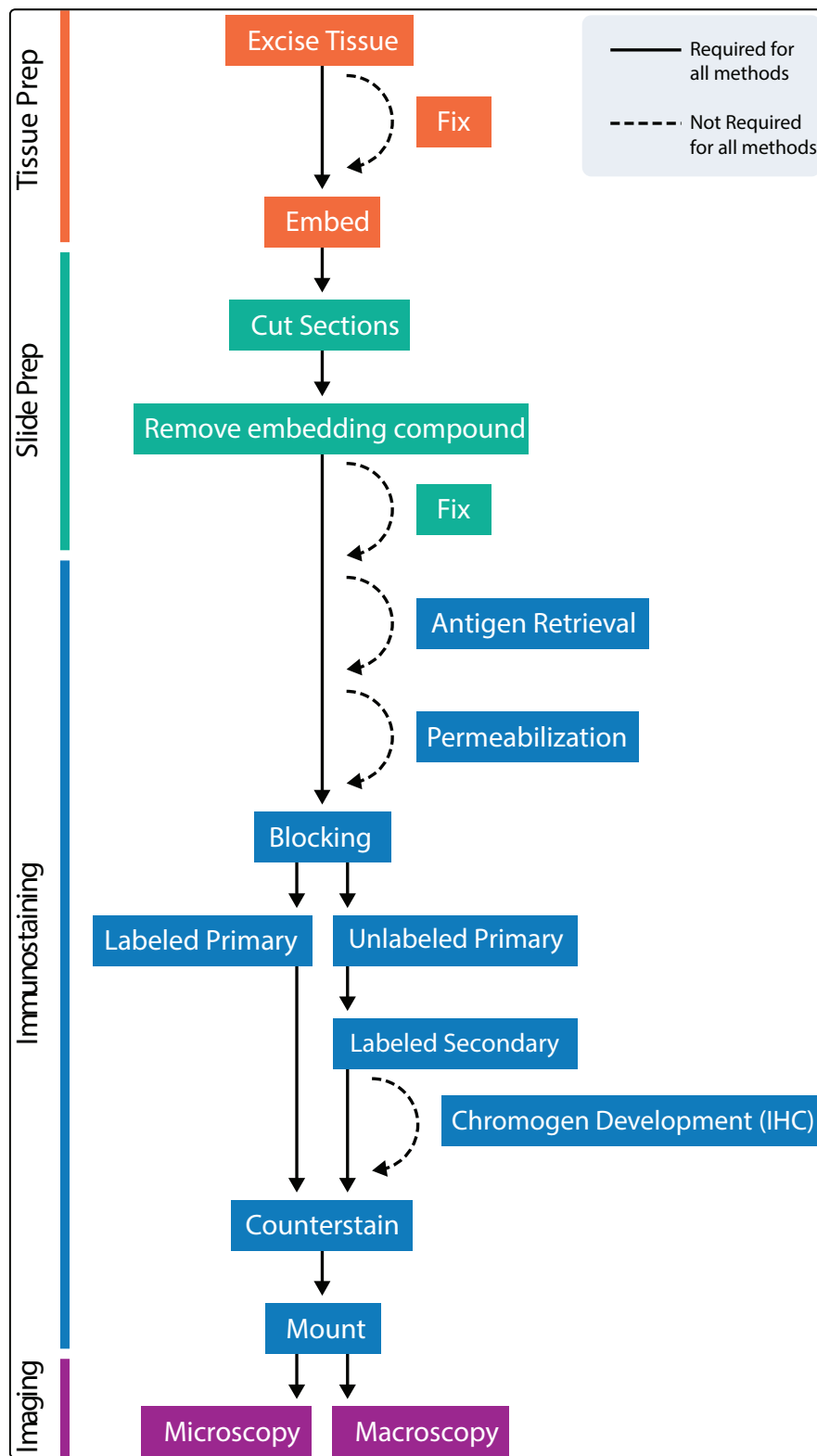


Figure 1: General protocol for preparing and staining tissue sections.

# Application Showcase

## I. Tissue Preparation

### 1) Fixation

The goal of fixation is to preserve the tissue's cellular structure as closely as possible to its native state.

To lessen risk of sample damage, it is suggested to test several fixative options to determine which fixative preserves both antibody binding and the structural integrity of the sample.

#### • Fixative Options

There are two common classes of fixatives: cross-linking fixatives and precipitating fixatives.

#### • Cross-linking fixatives

These fixatives act by creating covalent bonds between macromolecules in the tissue. Crosslinking can mask antigens, so these fixation methods are typically followed by an antigen retrieval step. The most common fixative in histology is formaldehyde gas dissolved in water.

#### • Precipitating fixatives

Alcohols are commonly used to fix frozen sections and smears. Alcohols permeabilize as they fix and do not induce cross-linking, eliminating the need for later permeabilization and antigen retrieval steps.

#### • Fixation Factors

While certain structures may be better preserved using specific fixation methods, there are several important factors to consider like pH, osmolarity, duration, tissue thickness, fixative volume and temperature.

### 2) Embedding

Tissue must be either fixed or frozen immediately after collection to prevent loss of tissue morphology and target protein degradation.

	Paraffin-Embedded	Frozen
Fixation	before embedding	After sectioning if needed
Sectioning Tool	Microtome	Cryotome
Viability	Years at room temperature	~1 year at -80 °C
Advantages	Preserves cell structures and proteins	Preserves enzyme activity, proteins remain in native state
Disadvantages	Toxic fixatives, proteins are denatured, fixation can shrink tissue and mask epitope	Vulnerable to rapid degradation, ice crystals can disrupt tissue structure

Table 1: Comparison between paraffin and frozen embedding approaches.

Tissues are typically preserved paraffin-embedded or frozen. Table 1 compares these two approaches.

## II. Slide Preparation

### 1) Cut Sections

For microscopy, sections are generally cut to a thickness of 4 to 10 µm so that the section is one cell thick.

Tissues of any thickness can be imaged on an Odyssey® M, Odyssey DLx, or Odyssey XF Imager. Optimal thickness depends on the tissue and embedding method.

A microtome or cryotome is used to cut thin slices of paraffin-embedded tissue or frozen tissue sections respectively.

Once cut, tissue sections are mounted on microscope slides and allowed to dry overnight prior to immunohistochemistry. Alternatively, sections can be transferred to well plates for free-floating section imaging.

### 2) Remove Embedding Compound

For microscopy, sections are generally cut to a thickness of 4 to 10 µm so that the section is one cell thick.

Tissues of any thickness can be imaged on an Odyssey® M, Odyssey DLx, or Odyssey XF Imager. Optimal thickness depends on the tissue and embedding method.

### 3) Free-Floating Sections

In free-floating immunohistochemistry, sections are not mounted until after the immunohistochemistry process is complete. Sections are stained while floating in solution, typically in a large-welled plate. Because the antibody can penetrate the tissue from all sides, thicker sections can be used compared to slide-mounted sections (20 to 50 µm).

# Application Showcase

## III. Immunostaining

### 1) Perform Antigen Retrieval

Fixation can alter protein biochemistry, causing the epitope of interest to be masked from the primary antibody by cross-linking of amino acids within the epitope or cross-linking with unrelated biomolecules at or near the epitope.

The process of epitope/antigen retrieval refers to unmasking the epitope to restore epitope/antibody binding. It should only be performed if necessary because harsh conditions, including acidic or basic pH and high temperatures, can cause the tissue to dissociate from the slide.

An epitope can be unmasked in several ways.

**Heat-induced epitope retrieval (HIER):** Epitopes are unmasked by heating the sections in a buffered solution. Citrate and EDTA-based buffers are commonly used. A variety of heating sources can be used, including a microwave, water bath, pressure cooker, or vegetable steamer. Epitope unmasking improves as temperature increases. Water baths and microwaves typically achieve temperatures of 100°C, while pressure cookers can reach up to 120°C.

**Proteolytic-induced epitope retrieval (PIER):** Enzymes such as trypsin, proteinase k, pronase, or pepsin are used to unmask the antigen.

**Room temperature epitope retrieval (RTIER):** Acid, typically formic acid (pH 2) or hydrochloric acid (pH 1), is used to reverse cross-linking.

### 2) Permeabilize

Permeabilization facilitates the entry of antibodies into the cells. The extent of permeabilization required depends on the target.

Permeabilization, like fixation, can affect the morphology of cells, including the antigen of interest.

Detergents commonly used for permeabilization include NP-40, Triton® X-100, Tween® 20, and saponin. After permeabilization, wash the slide in water or PBS.

### 3) Block

#### • Create a Hydrophobic Barrier

Prior to adding blocking solution or primary antibodies, draw a barrier on the slide around the tissue section using a hydrophobic pen. The barrier keeps reagents from flowing off the tissue section, allowing application of solutions directly to the slide in smaller amounts.

#### • Block Endogenous Biotin or Enzyme Activity

Blocking endogenous biotin or enzymatic activity may be needed depending on the detection method. To determine if supplemental blocking of enzymatic activity is needed, add chromogen substrate and/or labelled probe to a control tissue section after antigen retrieval. If endogenous levels of the enzyme produce staining, additional blocking is needed, as described below. This step is typically not needed for fluorescence detection.

#### • Block endogenous biotin

If you intend to use a secondary antibody conjugated to biotin, block endogenous biotin by incubating the tissue in unlabelled streptavidin or avidin, followed by an excess of unlabelled biotin. This will prevent off-target binding of your labelled streptavidin-conjugated secondary antibody.

#### • Block endogenous peroxidase

If horseradish peroxidase (HRP) is used for chromogen development, quench endogenous peroxidase by incubating slides in 0.3 to 3.0% (v/v) peroxide in methanol.

#### • Block endogenous alkaline phosphatase

If the secondary antibody is labelled with alkaline phosphatase (AP), endogenous AP activity can be blocked with the AP inhibitor levamisole at 1 mM concentration.

These blocking steps may interfere with primary antibody binding and can be performed after the primary antibody incubation and wash step if preferred.

# Application Showcase

## • Block Non-Specific Antibody Binding

Target detection can be improved by blocking the non-specific binding of antibody to the tissue section. Intercept® Blocking Buffer (TBS, PBS, or protein-free), BSA, milk, or serum are commonly used to reduce non-specific binding.

Add blocking buffer directly to each tissue section and incubate the slides in a humidified chamber to prevent drying. Each blocking solution will have specific incubation conditions.

## 4) Incubate With Primary Antibody

Dilute the primary antibody in the same blocking buffer used in the previous step. The addition of detergent helps prevent non-specific interactions. A concentration of 0.1 to 0.2% Tween® 20 is commonly used. Incubate slides in a humidified chamber to keep them from drying out. Most primary antibodies perform well when incubated overnight at 4°C. Some may also perform well at room temperature or 37°C for shorter incubation times.

For multiplexed target detection, be certain each primary antibody is derived from a different host species or subclass and is validated to confirm there is no cross-reactivity. If all antibodies have the same optimal incubation times and temperatures, they can be incubated simultaneously.

After incubating the primary antibody, wash the slides with a buffer containing detergent. Use the same buffer system as in the previous steps. TBS + 0.1% Tween 20 (TBS-T) is commonly used. If the primary antibody is conjugated to a fluorophore, no secondary antibody incubation is needed.

## 5) Incubate With Secondary Antibody

Dilute the secondary antibody in the same blocking buffer used in previous steps with the addition of detergent. A concentration of 0.1 to 0.2% Tween® 20 is commonly used.

For IRDye® Secondary Antibodies, the recommended starting dilution is 1:200. For VRDye™ Secondary

Antibodies, the recommended starting dilution is VRD Rec. Incubate slides in the humidified chamber to keep slides from drying out.

For detection of multiple targets, all secondary antibodies can be incubated simultaneously if they are compatible and will not bind each other.

### a. Fluorophore-Conjugated Antibodies

For multiplex detection, make sure fluorophores are compatible and that wavelengths are separated enough to prevent bleedthrough for specific detection of each. For example, the 488, 700, and 800 nm channels on the Odyssey® M Imager are far enough apart for specific detection, while the 488 and 520 nm channels are not. Also, consider that cellular autofluorescence is brightest in the visible wavelengths, so NIR fluorophores will give better sensitivity and reduced background.

### b. Enzyme-Conjugated Antibodies

When using secondary antibodies conjugated to an enzyme, such as HRP or AP, you will need to add a substrate. The enzyme breaks down the substrate into a visible precipitate that stains the tissue. The colour of the stain depends on the substrate used. The stain should be developed immediately after secondary antibody incubation and subsequent washes, as enzymes are not stable at room temperature. Stain development must be watched closely, and the reaction must be quenched as soon as staining is satisfactory.

### c. Biotin-Conjugated Antibodies

Biotin binds strongly to its ligands avidin and streptavidin. Targets labelled with biotin are often visualized by adding avidin or streptavidin conjugated to a fluorophore or enzyme, like HRP or AP, for chromogenic development, as described above.

## 6) Counterstain

Slides can be counterstained to visualize overall tissue morphology. Common fluorescent counterstains include nuclear stains, like DAPI, or fluorophore-conjugated phalloidin to stain F-actin.

# Application Showcase

Counterstains are typically performed during or after the secondary antibody incubation.

Visible counterstains for IHC include hematoxylin, nuclear fast red, and methyl green. These can be detected with the RGB channel on the Odyssey® M Imager.

## IV. Imaging

### 1) Mount

#### Fluorescent Detection

Mounting media can protect against physical damage of the sample and photobleaching of incubation is needed. fluorescent dyes. Some mounting media will solidify the coverslip on the slide, while others will remain liquid.

For liquid mounting media, the edges of the coverslip will need to be sealed with epoxy or clear nail polish. Mounting media is typically added directly to the slide. The coverslip is carefully placed on top to avoid creating air bubbles.

#### Visible Detection

Although visual stains are not recommended, for visible detection, dehydrate slides through a series of increasing concentrations of alcohols followed by xylenes and allow slides to air dry prior to mounting the coverslip. Clear, adhesive mounting media is typically used.

### 2) Image

Tissue sections can be imaged using the LICORbio Odyssey® M, Odyssey F, or Odyssey XF Imager.

Ensure slides are completely dry before imaging on an Odyssey® Imager to prevent the mounting media or sealant from damaging the scan surface.

LICORbio Odyssey Imagers include image acquisition and analysis software.

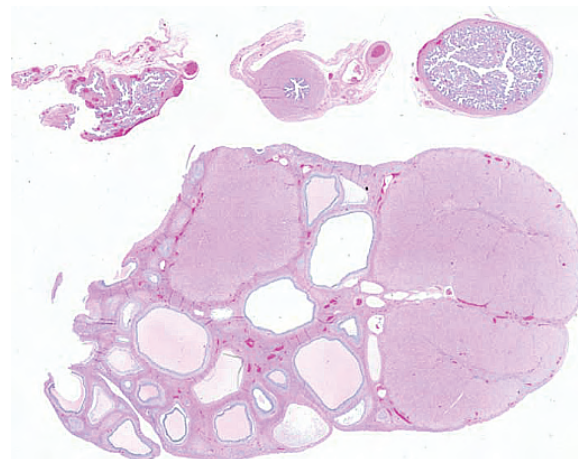


Figure 3: An example tissue section using a pig ovary. Ovaries were deparaffinized, stained using H&E stain, then imaged at 5 µm using the RGB Trans channel of an Odyssey® M Imaging System.



Figure 4: Swine intestine stained for DNA, β-Catenin, and MUC2. The tissue was stained for nuclei (NucSpot 488, blue), β-Catenin (anti-β-Catenin and IRDye® 680RD Goat anti-Mouse Secondary Antibody, red), and MUC2 (anti-MUC2 and IRDye® 800CW Goat anti-Rabbit Secondary Antibody, green) and imaged at 5 µm resolution on an Odyssey® M Imaging System.

## Conclusion

Odyssey M, Odyssey F, and Odyssey XF Imagers offer macroscopic imaging of tissue sections, allowing for detection of tissue- or region-specific localization and expression of targets. Additionally, these imagers can screen multiple tissue slides simultaneously, offering increased throughput for imaging.

The Odyssey M and Odyssey F Imagers can perform macroscopic imaging of multiple tissue section slides at once, allowing for high-throughput detection of tissue- or region-specific localization and expression of

# Application Showcase

targets. Additionally, Odyssey Imagers provide an industry-leading 6 logs of dynamic range, and the line

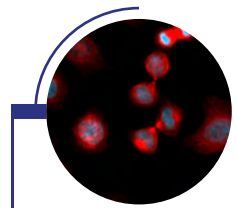
scanning technology of the Odyssey M delivers exceptionally fast acquisitions of tissue section images.

Instrument	Resolution	Channels
3-Channel Odyssey F	21 – 337 µm	<ul style="list-style-type: none"><li>• 700 nm (2 channels)</li><li>• 800</li></ul>
10-Channel Odyssey F	21 – 337 µm	<ul style="list-style-type: none"><li>• 488 nm (4 channels)</li><li>• 520 nm (3 channels)</li><li>• 700 nm (2 channels)</li><li>• 800 nm</li></ul>
Odyssey M	5 – 100 µm	<ul style="list-style-type: none"><li>• Onboard Chemi (Optional)</li><li>• RGB Transillumination (4channels)</li><li>• RGB Epi-illumination (4channels)</li><li>• 488 nm (4 channels)</li><li>• 520 nm (3 channels)</li><li>• 700 nm (2 channels)</li><li>• 800 nm</li></ul>

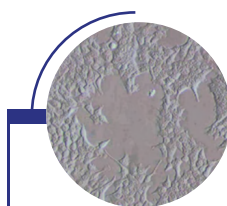
## LICORbio's Odyssey Imagers



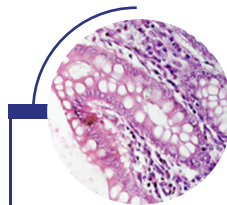
Odyssey® Family



**HeLa Kyoto cells**  
Multichannel fluorescence image



**Cos7 cells**  
Improved Hoffman modulation contrast



**Intestine**  
HE staining, brightfield contrast



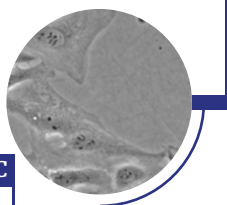
## Axiovert 5

Smart microscopy for your cell culture and research

- ★ Be smart:  
Simply focus and snap to get crisp images for documentation.
- ★ Stay flexible:  
Use all standard contrasting techniques in transmitted light and combine them with multichannel fluorescence.
- ★ Relax:  
Clever features make your work easier. Use Axiovert 5 as a standalone and save your images on USB.



Transmitted light image,  
Objective:  
LD A-Plan 40x/0.55 Ph 1  
**U2OS cells in phase contrast**

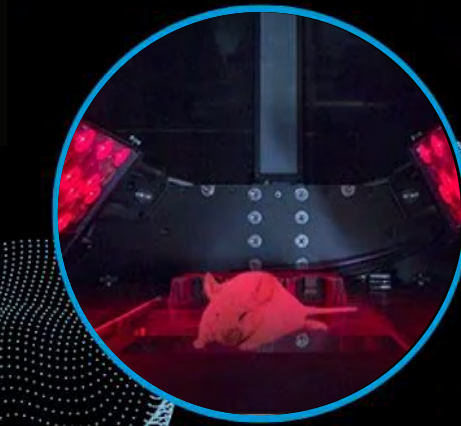


**Cells in transmitted light PlasDIC**



**Cells in transmitted light DIC**

# Application Showcase



## Exploring applications of *in vivo* NIR-II imaging in preclinical research

### Disrupting preclinical research with Photon etc IR VIVO NIR II Preclinical Imager

Preclinical optical imaging suffers from the inability to localize signals due to light absorption, scattering and autofluorescence in living tissues. *In vivo* optical imaging can localize a signal well when it is at the surface but not when it is deep in the organism. The emergence of NIR-II offers a promising solution. NIR-II *in vivo* imaging is not impacted in the same way by drawbacks of light propagation in living tissues, thus enabling real-time imaging of optical probes much deeper in the organism and with much higher resolutions.

### Introduction

The second near-infrared spectral region (NIR-II) also referred to as shortwave infrared (SWIR) is usually defined as the wavelength range from 900 to 1700 nm.

A full understanding of why this spectral window works so well for *in vivo* imaging remains to be fully elucidated<sup>1</sup>, but a few principles are clear: SWIR emitters are excited by NIR-I light which has a better penetration, and there is less autofluorescence, scattering and absorption of light in the NIR-II wavelengths of 1000 to 1700 nm, as shown in Figure 1.

**Keywords:** NIR-II imaging, preclinical, near-infrared, tumour, vascular, therapeutic

# Application Showcase

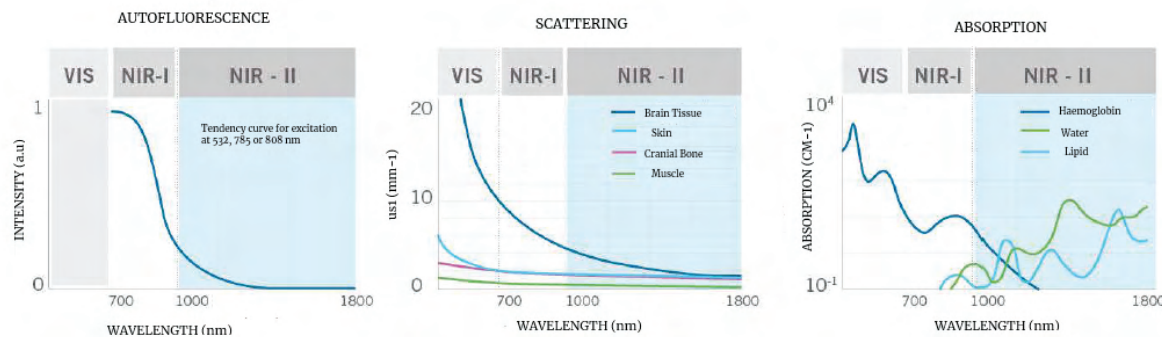


Figure 1: The weaker autofluorescence by the tissues in the NIR-II window contributes to enhancing the signal – to – background ratio. The reduced scattering and minimal absorption of emission signals by the tissues helps to improve spatial resolution and depth penetration, which can be up to 10x better.

## Preclinical applications

NIR-II imaging is poised to bring us an unprecedented combination of fast, deep and high-resolution imaging at a lower cost. This will have the effect of bringing preclinical imaging techniques such as visualizing tumours, vascular anatomy, and contact-free cardiography to institutes that do not have access to more costly micro-MRI or micro-CT imaging systems. Here is a review of some of the basic preclinical applications made possible by the new modality.

### Visualizing blood vessels & mapping blood flows

In vivo real-time visualization of the vascular system has great potential to improve our understanding of circulatory system-related pathologies and angiogenesis due to its ability to image vascular anatomy and blood flow. Current methods for assessing vascular structures such as micro-computed tomography (micro-CT), magnetic resonance imaging (MRI), have the advantage of unlimited penetration depth but suffer from long acquisition times and post-processing times thus complicating real-time imaging in the small animal. NIR-II imaging is also nicely suited to map arterial and venous blood flows even beyond the abilities of ultrasound at lower velocities<sup>2</sup>. Such blood flow mapping could help to model tumour hemodynamics and oxygenation. Moreover, these capabilities are relevant for functional imaging of activity states such as muscle motion or brain response to stimuli, which are closely linked to perfusion. Murine hindlimb models have been

extensively used to look at the angiogenic effects of blood vessel growth modulation in healthy and diseased tissues such as animal models of peripheral artery disease. The high-resolution imaging of the blood vascular network will be useful for visualizing hindlimb ischemia and assessing the effectiveness of angiogenic therapies.

Assessing the effectiveness of angiogenic modulation is also important for cancer research. A solid tumour with a diameter of over 1 mm requires an adequate blood supply for growth and metastasis. Early detection and therapy research should also have an efficient and simple method to monitor tumour angiogenesis and NIR-II could represent the answer at an economical price point.



Figure 2: Data from an experiment mouse that had Ovarian tumour (SKOV-3) in the left flank following an IV injection of PBS QDots that have peak emission 1300 nm. The negative contrast in the tumour indicates a tumour barrier preventing contrast perfusion into the tumour. We also clearly see the blood vessels feeding the tumour.

Image courtesy of the Preclinical Imaging Laboratory of the National

# Application Showcase

## Visualizing tumours

Early detection research will also benefit from seeing tumours earlier in the small animal. As previously mentioned, bioluminescence and fluorescence imaging have the advantage of sensitivity and detecting small changes in tumour biology, but these techniques have replaced the calliper mostly in xenograft studies where the tumour is at the surface. Visualization of tumours is possible with positive contrast caused by passive targeting (e.g. EPR effect or targeting via lymph nodes), receptor binding, or probes activated by lysosomal enzymes. More recently, HER2-amplified breast cancer BT474 cells brain parenchyma was imaged, following IV administration of Licor's IRDye800 conjugated to trastuzumab (Figure 3).

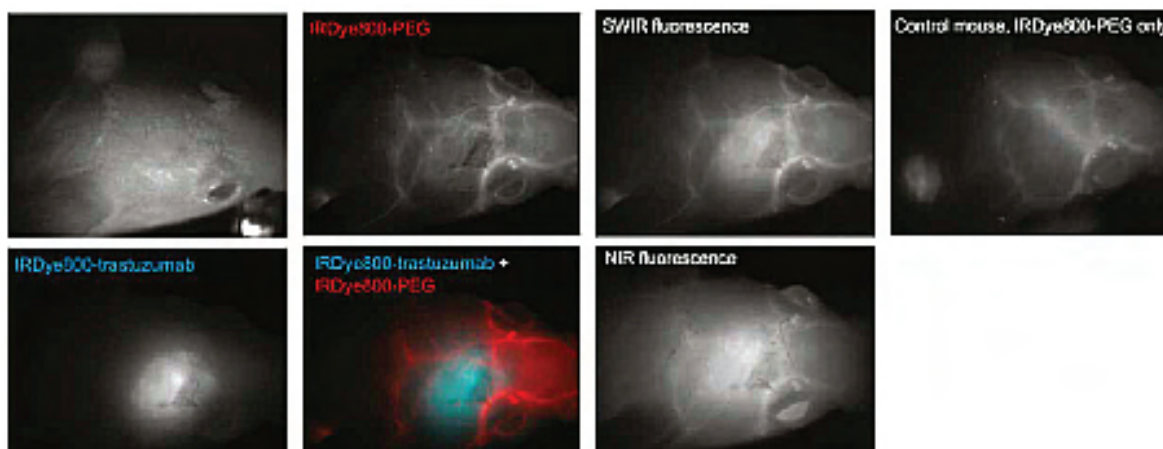


Figure 3: Targeted SWIR imaging *in vivo* with IRDye 800CW of a nude mouse with a brain tumour from implanted human BT474 breast cancer cells. Three days after injecting IRDye 800CW-trastuzumab conjugate, fluorescence from the labelled tumour was imaged noninvasively through skin and skull on a SWIR camera<sup>3</sup>.

In addition, a PEGylated version of the Licor dye was used to show the blood vessels surrounding the tumour<sup>3</sup>.

## Contact-free measurements of cardiography, respiratory rate & intestinal contractions

High-speed imaging made available by the fast frame rates of InGaAs cameras allows for contact-free cardiography and respiratory rate measurements in both anesthetized and awake animals. Using a blood

pool contrast agent-based in micellar InAs–CdSe–CdS, short-wave infrared quantum dots with high quantum yield have generated sufficient signal-to-noise ratio for both anesthetized and awake mice showing how physiology is deeply influenced by anesthesia<sup>4</sup>.

Such contact-free measurements of awake mice were obtained without the use of any restraining device. The monitoring of heart and respiratory rates of an anesthetized mouse was also recently observed by Photon etc. scientists in partnership with the Preclinical Imaging Laboratory of the National Research Center in Ottawa. This study also measured the mouse's intestinal contractions, values that were corroborated by scientific publications (Figure 4).

## Real-time monitoring of *in vivo* targets for therapeutics development

NIR-II imaging has the potential to fundamentally impact the development of targeted therapeutics and drug discovery with real-time pharmacokinetic imaging of over a thousand targets simultaneously in a single mouse. The new NIR-II imaging technologies are now designed to offer the time profiling analysis for each pixel or a region of interest (ROI) in a single click, hence obtaining rapidly the real-time kinetic curves at several locations simultaneously on the mouse (Figure 5). Then, a principal component analysis (PCA) may be applied to a time series of fluorescence imaging to precisely delineate major tissues and organs.

# Application Showcase

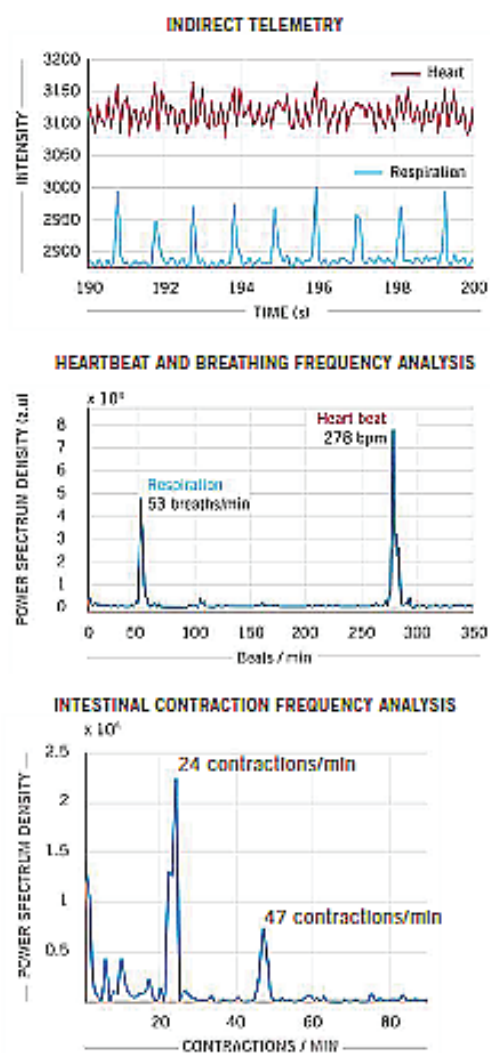


Figure 4: Real-time imaging data on heartbeat, respiratory rate and intestinal contractions obtained on Photon etc.'s IR VIVO reflect values found in the literature.

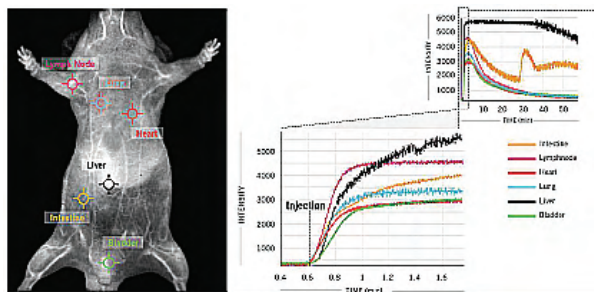


Figure 5: In this example, 6 clicks were used to obtain kinetic curves at 6 different locations - intestine, lymph nodes, heart, lung, liver, bladder on the mouse's body for a one-hour scan following ICG injection in a male CD1 mouse.

With one click spectrum extraction, it is possible to measure the kinetics of fluorescent intensity changes allowing scientists to determine the accumulation and elimination of the probes in selected regions or organs and to compare relative signal ratios between the organs. This information helps understand how the probes are metabolized by the biological system in detail and to obtain values from hepatobiliary elimination and gastrointestinal transit rates. Such a wealth of biodistribution data from a single mouse should be of great interest to the probe development community. Historically, near-infrared imaging has been used with NIR dyes conjugated to anticancer agents for probe development. Such programs could be enhanced by simply shifting the detection technology to NIR-II and without relying on organ extraction to determine the biodistribution (Figure 6).

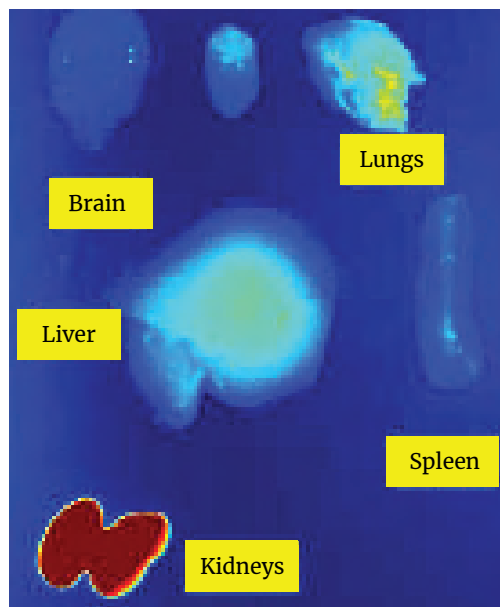


Figure 6: Studies ex vivo won't be necessary anymore to get the biodistribution data in each organ. Image courtesy of the Preclinical Imaging Laboratory of the National Research Center in Ottawa

Using the same animal for multiple PK analyses will also help to further reduce cohort sizes for preclinical studies. NIR-II could start to play a fundamental role in compound screening and allow researchers to use in vivo imaging earlier in the process of probe validation.

# Application Showcase

One-way NIR-II in vivo imaging will undoubtedly affect preclinical workflow is in study design, especially as it relates to the validation of probes in preclinical testing (Figure 7). With NIR-II in vivo imaging, it is possible to look at very small concentrations of probes flow through different ROIs of an organism and to track minute changes in real-time.

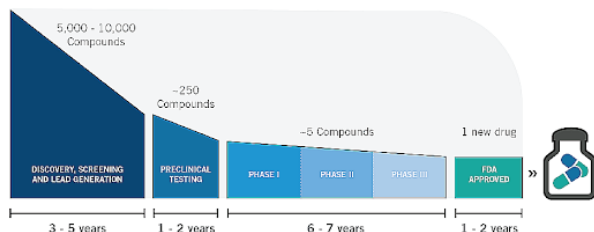


Figure 7: Therapeutics drug development timeline.

## Conclusion

NIR-II imaging has tremendous potential in preclinical optical imaging. The unique properties of near – infrared spectral region aids this technology, enabling deeper tissue penetration, higher resolution and real – time visualisation of biological processes. Photon etc's IR VIVO NIR II Preclinical Imager takes advantage of latest developments in SWIR imaging to deliver clear quantitative images.

## References

1. Zhu, S.; Yung, B. C.; Chandra, S.; Niu, G.; Antaris, A. L.; Chen, X. Near-Infrared-II (NIR-II) Bioimaging via Off-Peak NIR-I Fluorescence Emission. *Theranostics* 2018, 8 (15), 4141–4151. DOI: 10.7150/thno.27995.
2. Hong, G.; Lee, J. C.; Robinson, J. T.; Raaz, U.; Xie, L.; Huang, N. F.; Cooke, J. P.; Dai, H. Multifunctional in Vivo Vascular Imaging Using Near-Infrared II Fluorescence. *Nature Medicine* 2012, 18 (12), 1841–1846. DOI: 10.1038/nm.2995.
3. Carr, J. A.; Franke, D.; Caram, J. R.; Perkinson, C. F.; Saif, M.; Askoxylakis, V.; Datta, M.; Fukumura, D.; Jain, R. K.; Bawendi, M. G.; Bruns, O. T. Shortwave Infrared Fluorescence Imaging with the Clinically Approved Near-Infrared Dye Indocyanine Green. *Proceedings of the National Academy of Sciences* 2018, 115 (17), 4465–4470. DOI: 10.1073/pnas.1718917115.
4. Bruns, O. T.; Bischof, T. S.; Harris, D. K.; Franke, D.; Shi, Y.; Riedemann, L.; Bartelt, A.; Jaworski, F. B.; Carr, J. A.; Rowlands, C. J.; Wilson, M. W. B.; Chen, O.; Wei, H.; Hwang, G. W.; Montana, D. M.; Coropceanu, I.; Achorn, O. B.; Kloepper, J.; Heeren, J.; So, P. T. C. Next-Generation in Vivo Optical Imaging with Short-Wave Infrared Quantum Dots. *Nature Biomedical Engineering* 2017, 1 (4). DOI: 10.1038/s41551-017-0056.



IR VIVO benefits from reduced light scattering, absorption and auto-fluorescence with a sensitive detection system in the near and shortwave infrared.

# Viscometer

Precise and Reliable

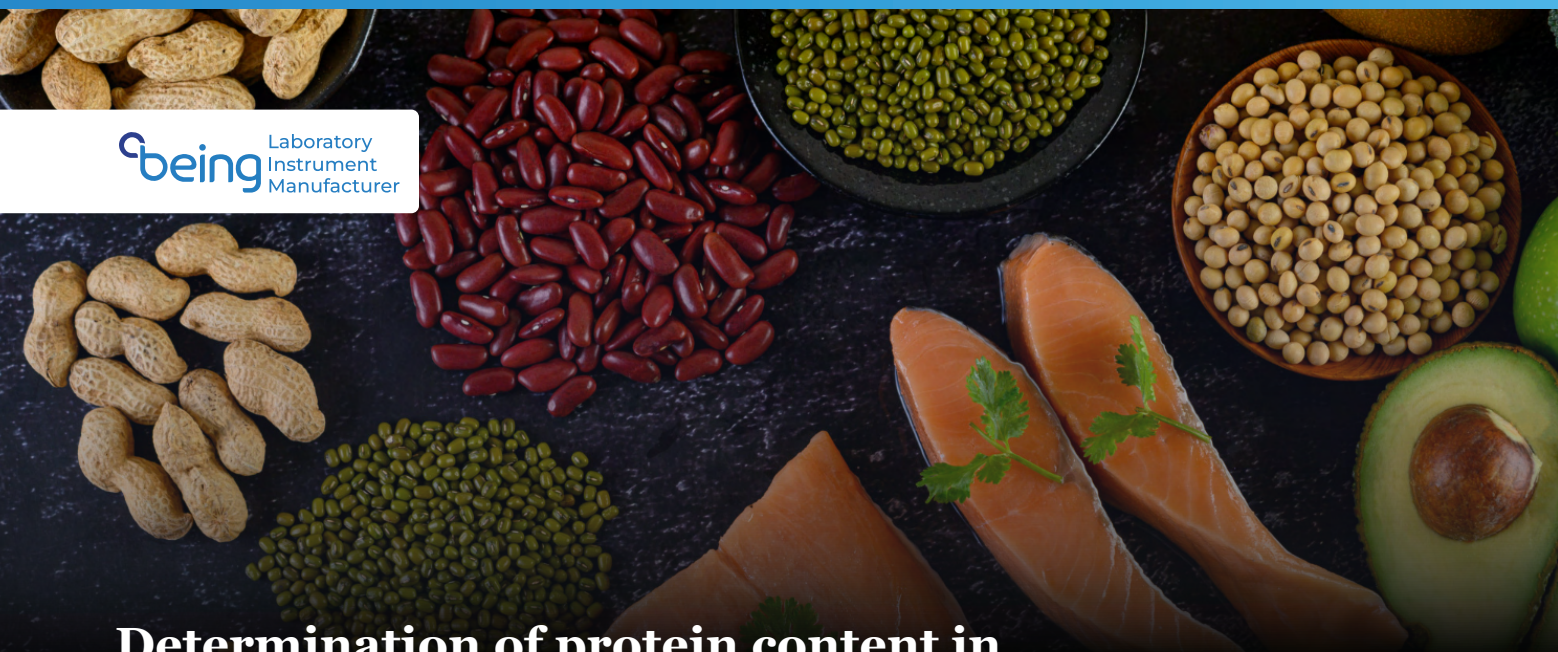
- Metal lifter
- Built – in RTD temperature probe
- Continuous value display
- Suitable for low, medium and high viscosity measurements
- Choose RPM according to your application



**cbeing** Laboratory  
Instrument  
Manufacturer

# Application Showcase

**being** Laboratory Instrument Manufacturer



## Determination of protein content in soybeans by Kjeldahl method

### Employing the BEING BPK-9870A Automatic Kjeldahl Nitrogen Analyzer

**P**rotein and nitrogen are two of the most fundamental building blocks of life. Proteins perform a wide range of important functions, from catalysing enzymatic reactions to mediating immune responses. A core structural feature that exists in all amino acids; the makers of proteins- is the presence of nitrogen. This elevates the importance of accurate measurement of protein and nitrogen across various sectors.

This is where the Kjeldahl method, a real workhorse originating in 1883 by Johan Kjeldahl, comes into play. Despite its long history, the Kjeldahl method is still applied in todays' labs to determine nitrogen content in organic substances as it provides reliable and versatile results. In the field of such determinations BEING's BPK-9870A Automatic Kjeldahl Nitrogen Analyzer reaches new levels of precision and safety.

**Keywords -** Kjeldahl method, protein analysis, soybeans, BEING BPK-9870A Automatic Kjeldahl Nitrogen Analyzer

### Introduction

Johan Kjeldahl developed the Kjeldahl method at the Carlsberg Laboratory in Copenhagen. It was initially invented for use in the brewing industry, though the Kjeldahl method's applications have expanded greatly since then. Today, the Kjeldahl method is used for determining nitrogen levels in a wide array of organic substances such as foods, beverages, and meat as well as agricultural products. It's even used to measure nitrogen levels in animal feed, waste products, environmental water and soil samples, biological materials, dairy products and pharmaceuticals.

The Kjeldahl method for total nitrogen determination has been improved and automated over the years but its principle have remained the same.

The method is divided into three main parts: digestion, distillation and titration. The determination of protein content starts by conversion of organic nitrogen present

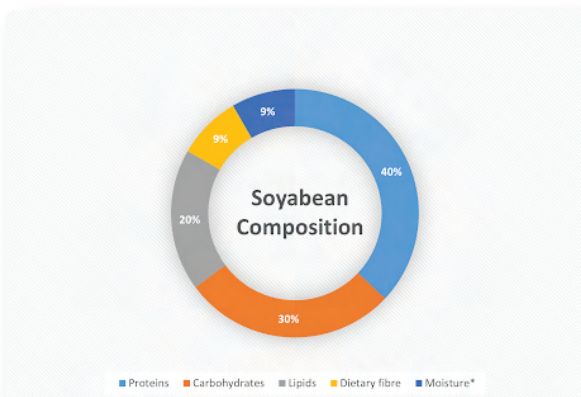
# Application Showcase

in samples to ammonium ions that can be easily measured, with subsequent titration analysis. Protein is expressed as percent by multiplying the nitrogen result by a factor that derives from the average nitrogen content of proteins (this factor varies according to the sample chosen).

This article explores the procedure for determination of protein content in soybeans using BEING's BK-9870A Automatic Kjeldahl Nitrogen Analyzer.

Soybeans (*Glycine max* (L.) Merr.), a legume species, originally from China, were introduced for commercial cultivation in India in the late 60s<sup>1</sup>. In less than a decade, soybeans have contributed significantly to India's oilseed production. Soybeans can be consumed in many forms as fermented foods (miso, tempeh, natto and soy sauce) and unfermented foods (tofu, soymilk, edamame, soy nuts and sprouts).

Soybeans are a rich source of plant-based protein and oil. On an average, they contain 40%–50% protein and 18% oil (Figure 1).



Moisture\* content based on the dry weight of soybean seeds.

Apart from being a rich source of proteins, these legumes possess bioactive compounds such as isoflavones, phytic acid and saponins. Based on the solubility, the soybean proteins are classified into water-soluble albumins, salt-soluble globulins, dilute acid/alkali-soluble glutelins, and alcohol-soluble prolamins.<sup>2,3</sup>

Efficient and accurate evaluation of protein content of foods is essential for determining their nutritional and economic value.

## Experimental

### Sampling

Nine varieties of soybeans were collected, and triplicates were performed to arrive at the mean value.

### Method

The study for protein content determination was conducted using the BEING BPK-9870A Automatic Kjeldahl Nitrogen Analyzer. All chemicals were purchased from Sigma Aldrich and used without further purification. About 0.5 g of each seed variety was weighed and transferred into 250 mL digestion tubes, where 20 mL of concentrated sulfuric acid and two tablets of catalysts, each containing 5 g  $K_2SO_4$  and 0.5 g  $CuSO_4 \cdot 5H_2O$ , were added. Digestion was carried out at 400°C for 3 h in BRJX-8B Digestion System. The samples were neutralised in BZH-1B Acid-Alkali Neutralization Unit. The digested samples were treated with 32% NaOH and the resulting ammonia was distilled in BPK-9870A Automatic Kjeldahl Nitrogen Analyzer. In a known volume of standardized 0.1 N  $H_2SO_4$ . Nitrogen content was determined by titration with a standardized 0.1 N HCl solution using a mixture (5:1) of bromocresol green and methyl red as an indicator. The crude protein content was estimated by multiplying the nitrogen content with the conversion factor 6.25. This conversion factor is universally accepted figure based on two assumptions a) all proteins have nitrogen content of 16%, thus  $100/16 = 6.25$  and b) all organic nitrogen originates from proteins.

The percentage of protein content in the nine soybean seed varieties are shown in table 1.

# Application Showcase

Sample variety	Protein %
JS- 335	40
JS71-05	39
PK- 564	41
JS90-41	41
JS75-46	38
NRC-2	39
MACS58	39
Monetta	39
MACS 13	38

Table 1: Percentage of protein content in sample soybean seeds.

## Conclusion

With the growing question of purity of foods, protein analysis aims to delve into nutritional and economic value of food products. The high accuracy, versatility, reproducibility and universal acceptance has made the Kjeldahl method indispensable for determining protein and nitrogen content in organic matter.

Efficient and accurate evaluation of protein content of foods is essential for determining their nutritional and economic value.

## References

1. <https://iisrindore.icar.gov.in/statistics.html>
2. Qin, P.; Wang, T.; Luo, Y. A Review on Plant-Based Proteins from Soybean: Health Benefits and Soy Product Development. *Journal of Agriculture and Food Research* 2022, 7 (7), 100265. DOI: 10.1016/j.jafr.2021.100265.
3. Friedman, M.; Brandon, D. L. Nutritional and Health Benefits of Soy Proteins. *Journal of Agricultural and Food Chemistry* 2001, 49 (3), 1069–1086. DOI: 10.1021/jf0009246.



## BPK-9870A Automatic Kjeldahl Nitrogen Analyzer

# Protocol: Quantitative Western Blot Analysis with replicate samples

Replicate measurements are critical for quantitative Western blot (QWB) analysis. The purpose of QWB analysis is to monitor changes in the relative abundance or modification of a target protein within a group of samples. Does the experimental treatment cause an increase or decrease in target abundance, compared to the untreated or control condition?

Replicate samples confirm the validity of observed changes in protein levels. Without replication, it is impossible to know if an effect is real or simply an artifact of experimental noise or variation.

## Types of Replicate Measurements

**Technical replicates** are repeated measurements used to establish the variability of a protocol or assay and determine if an experimental effect is large enough to be reliably distinguished from the assay noise.

**Biological replicates** are parallel measurements of biologically distinct and independently generated samples, used to control for biological variation and determine if the experimental effect is biologically relevant. The effect should be reproducibly observed in independent biological samples.

## Reporting Changes in Relative Abundance

QWB uses ratiometric analysis: This compares the intensity of a target protein band to a control sample's band, providing a relative abundance measure.

**Normalisation is key:** Normalize your QWB data using an appropriate internal loading control (such as total protein staining). Normalization mathematically corrects for small, unavoidable variations in sample loading and transfer by comparing the target protein to an internal loading control.

**Calculate the ratio:** The normalized signal intensity of the target band in each sample should be divided by the normalized intensity of the target band in the control sample.

The resulting ratios, expressed as fold change or percentage (%) change, are used to compare relative protein levels across the samples on your blot. Because all samples are compared to the control, these measurements are proportional and are independent of raw signal intensity.

**Fold change** is a unitless value that compares the relative abundance of a target protein to the control sample on the same membrane.

A value above 1.0 indicates an increase in abundance relative to the control; a value below 1.0 indicates decreased abundance (Table 1).

$$\text{Fold change} = \frac{\text{normalized signal}_{\text{SAMPLE}}}{\text{normalized signal}_{\text{CONTROL}}}$$

# Tech Corner

Percentage (%) change is a unitless value like fold change that expresses changes in relative abundance as a percentage.

A positive percentage indicates increased abundance relative to the control; a negative percentage indicates decreased abundance (Table 1).

$$\% \text{ change} = \left( \frac{\text{normalized signal}_{\text{SAMPLE}}}{\text{normalized signal}_{\text{CONTROL}}} - 1 \right) \times 100\%$$

Fold Change	% Change
1.00	0
1.20	0.20
1.50	0.50
2.00	1.00
0.80	-0.20
0.50	-0.50
0.10	-0.90

Table 1: Relative abundance of target protein, expressed as fold change and % change

## Experimental Design

### Analysis of Replicate Samples on Separate Western Blot

Plan an appropriate strategy

Collect replicate data. A minimum of three replicates should be performed for each sample, including the controls.

Use this protocol to analyse and compare replicate samples on separate Western blots

Samples should be loaded in random order on each blot to minimize position effects. Sample placement on the blot (for example, in edge lanes vs. interior lanes) may affect signal intensity and introduce variability. Random sample placement will reduce the impact of position effects.

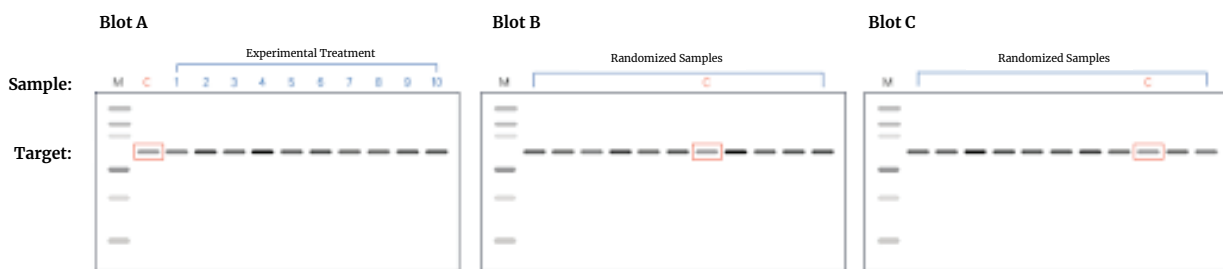


Figure 1: Replicate blot layout described in this protocol. Each gel is loaded with MW marker (M), control sample (C), and experimental samples (1-10). On blots B and C, control and experimental samples are loaded in random order.

## Quantitative Western Blot Normalization

Normalize your Western blot data, using an appropriate internal loading control

Use the normalized band intensity values for analysis of technical or biological replicates

### Calculations for Replicate Analysis

**STEP 1:** Prepare an analysis spreadsheet with the normalized band intensity values for each replicate

Western blot data must be normalized BEFORE replicate analysis is performed.

**STEP 2:** Using the normalized values, calculate the fold change (ratio of the experimental sample to the control) for each sample on replicate blot A (depicted in Figure 2).

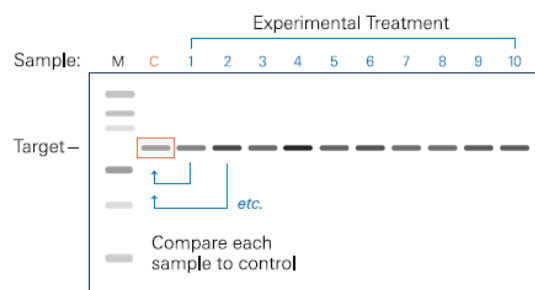


Figure 2. Fold change calculations: example data for Blot A. (top) In the blot diagram, C indicates the untreated control sample. Samples 1-10 received the experimental treatments. M indicates molecular weight marker. (right) Fold change was calculated for each band, using the normalized intensity values from Blot A. Each experimental sample is compared to the control, to generate a ratio. Example values are shown for illustration.

Sample	Target, norm. intensity	Control, norm. intensity	Fold change
C	10,000	10,000	1.00
1	9000	10,000	0.90
2	12000	10,000	1.20
3	15000	10,000	1.50
4	17000	10,000	1.70
5	23000	10,000	2.30
6	16000	10,000	1.60
7	18000	10,000	1.80
8	14000	10,000	1.40
9	13000	10,000	1.30
10	12000	10,000	1.20

**STEP 3:** Repeat the fold change calculations with the normalized values from replicate blots B and C (depicted in Figure 3).

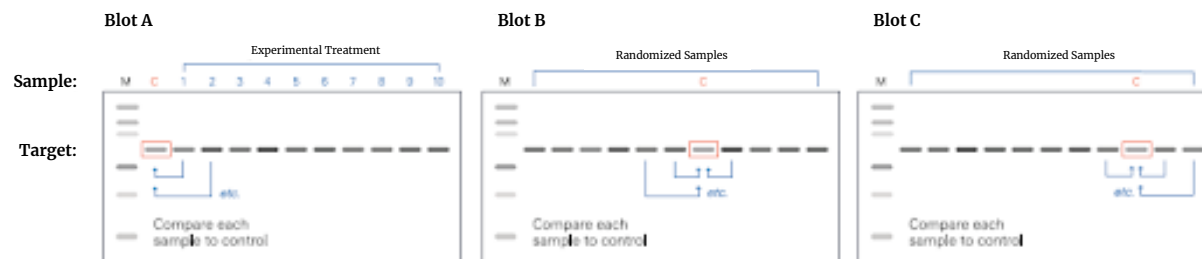


Figure 3. Fold change calculations. Example data are shown for Blots A, B, and C. (top) Strategy for calculating the fold change. (Left) Fold change values for the three blots. In this illustration, samples 1 - 10 were loaded on replicate blots (Blots A, B, and C are technical replicates).

Sample	Blot A fold change	Blot B fold change	Blot C fold change
C	1.00	1.00	1.00
1	0.90	1.00	1.10
2	1.20	0.90	0.80
3	1.50	1.80	2.30
4	1.70	1.50	1.20
5	2.30	2.60	3.00
6	1.60	1.30	1.80
7	1.80	1.60	1.50
8	1.40	1.20	1.30
9	1.30	1.60	1.20
10	1.20	1.50	1.80

**STEP 4:** Using the fold change values from each replicate blot -

- Calculate the mean fold change of each replicate measurement

$$\text{Mean fold change} = \frac{\text{sum of replicate values for an experimental sample}}{\text{number of replicates for that sample}}$$

- Calculate the standard deviation of the fold change for each replicate measurement
- Calculate the coefficient of variation (CV) of the fold change for each replicate measurement.

$$CV = \frac{\text{standard deviation of fold change for replicates}}{\text{mean fold change of replicates}} \times 100\%$$

**STEP 5:** Plot the fold change in protein expression as a function of the treatment (Figure 4).

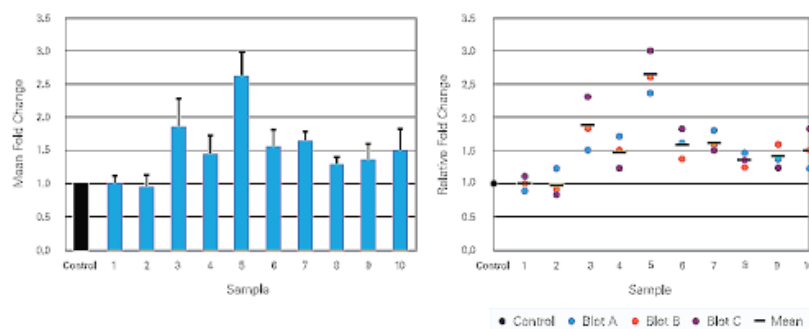


Figure 4. Bar graph and scatterplot of the fold change data in Table II. (left) Mean fold change was plotted for each sample on a bar graph. Error bars indicate the standard deviation for each measurement ( $n = 3$ ). The control is indicated by a black bar. (right) Fold change values from all blots were displayed as a scatterplot. The mean fold change for each sample is indicated by a horizontal line. The control sample is represented by a black dot. Technical replicates of samples 1–10 are shown ( $n = 3$ ).

## Data Interpretation

Use the fold change and % change values for relative comparison of samples.

% change and CV can be used to evaluate the robustness of your QWB results

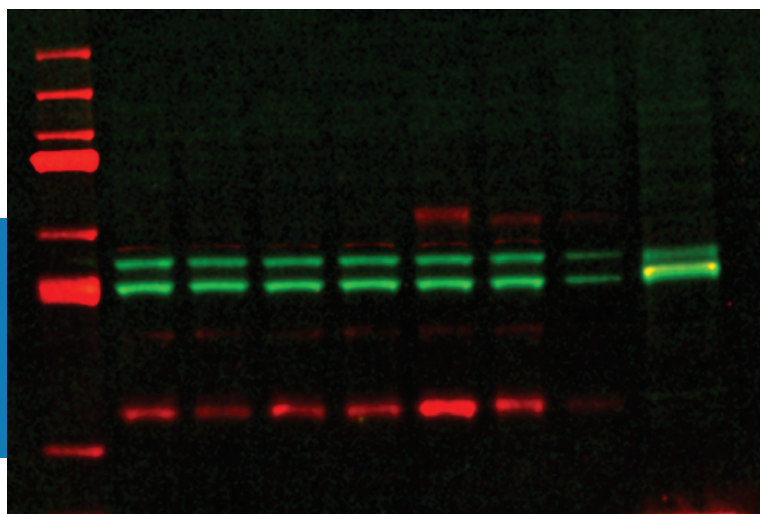
On a Western blot, a change in band intensity is meaningful only if the magnitude of the % change substantially exceeds the CV (Table 3).

The coefficient of variation (CV) describes the spread or variability of measured signals by expressing the standard deviation (SD) as a percent of the mean. Because CV is independent of the mean and has no unit of measure, it can be used to compare the variability of data sets and indicate the precision and reproducibility of an assay.

- A low CV value indicates low signal variability and high precision of measurement.
- A larger CV indicates greater variation in signal and reduced precision

Sample	Blot A fold change	Blot B fold change	Blot C fold change	Mean fold change	% change	Std. deviation	CV
C	1.00	1.00	1.00	1	0%	0	0%
1	0.90	1.00	1.10	1	0%	0.1	10%
2	1.20	0.90	0.80	0.97	-3.00%	0.21	22%
3	1.50	1.80	2.30	1.87	87%	0.4	22%
4	1.70	1.50	1.20	1.47	47%	0.25	17%
5	2.30	2.60	3.00	2.63	163%	0.35	13%
6	1.60	1.30	1.80	1.57	57%	0.25	16%
7	1.80	1.60	1.50	1.63	63%	0.15	9%
8	1.40	1.20	1.30	1.3	30%	0.1	8%
9	1.30	1.60	1.20	1.37	37%	0.21	15%
10	1.20	1.50	1.80	1.5	50%	0.3	20%

Table 3. CV and reported % change. The observed change in sample 2 (blue) is smaller than the CV of the measurement and is not meaningful. In samples 8, 9, and 10 (green), the reported change exceeds the CV by at least 2.5X. These changes are likely to be significant. Technical replicates of samples 1-10 are shown (n = 3).



# Product Highlight

## Surface Plasmon Resonance: Affinitè Instruments

### What is SPR?

Surface plasmon resonance (SPR) is an optical, surface-sensitive technique used to study the label-free interaction of biomolecules in a complex environment in real-time.

In a typical SPR experiment, ligands are immobilized on a SPR sensor surface which is exposed to a flowing solution of analytes in a microfluidic channel. The sensor surface is generally a glass prism covered with a thin metal layer, like gold or silver. A plane-polarized, monochromatic incident light is directed onto the sensor to which the ligands are attached, creating charged oscillations, called surface plasmons, at the metal surface.

When analytes become bound to surface-immobilized ligands, the surface plasmon resonance conditions change, resulting in a change in the reflected angle or wavelength of the light, depending on the interrogation used. This change is captured and plotted vs. time to generate a sensogram.

Sensograms are used to extract affinity and kinetic data of the interactions between the ligand and analyte. They can also reveal any specificity and concentration information through the magnitude of the SPR signal. In general, a sensogram has five phases:

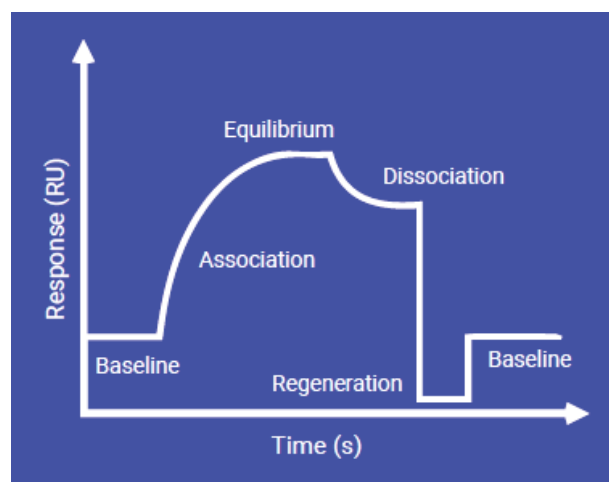
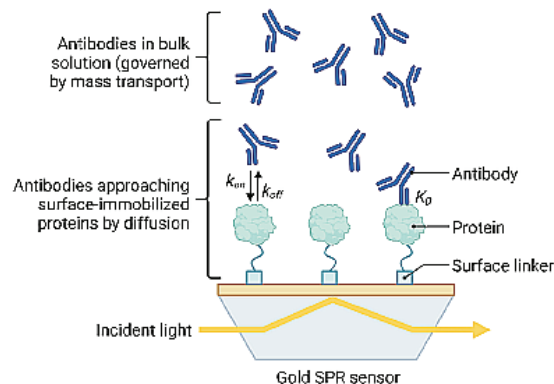
**Baseline:** The initial phase is the baseline.

**Association:** The second phase is where analytes begin to bind to immobilized ligands.

**Steady state:** This phase occurs at the top flat portion of the sensogram where the net rate of bound analytes is zero.

**Dissociation:** This phase begins when the analyte solution is replaced by a wash buffer, which causes the specific interactions between the analytes and ligands to break.

**Regeneration:** Finally, a low pH buffer such as glycine is flowed to reset the SPR baseline signal as the beginning of the experiment.



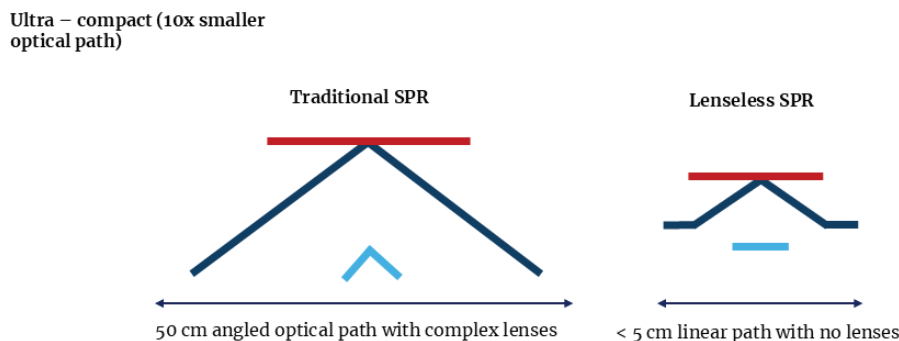
# Product Highlight

## Why Lenseless SPR® Technology?

In traditional Surface Plasmon Resonance (SPR) systems, angular interrogation is utilized to generate the SPR signal, requiring an angled optical path of approximately 50 cm. This method employs complex and delicate lenses to ensure proper focusing of light onto the sensing surface and then collection onto the detector.

*Lenseless SPR systems feature a linear optical path that is approximately 10 times shorter than that of traditional SPR systems.* This linear path eliminates the need for lenses, thereby offering the potential to significantly reduce the size of the main components of the SPR system, making it ultra-compact.

Affinité's Lenseless SPR® Technology streamlines the traditional complexities, by achieving a more compact and efficient design, making it easier than ever to harness the power of SPR.



## Affinité's Compact and Innovative Solution

P4SPR 2.0



P4PRO  
and  
Affipump



P4PRO+



## Key Features

- **Lenseless SPR® Technology**
- **Compact and Flexible Instruments**
- **Integrated Microfluidics**
- **One Instrument, Infinite Possibilities**
- **Lower Operating Costs**

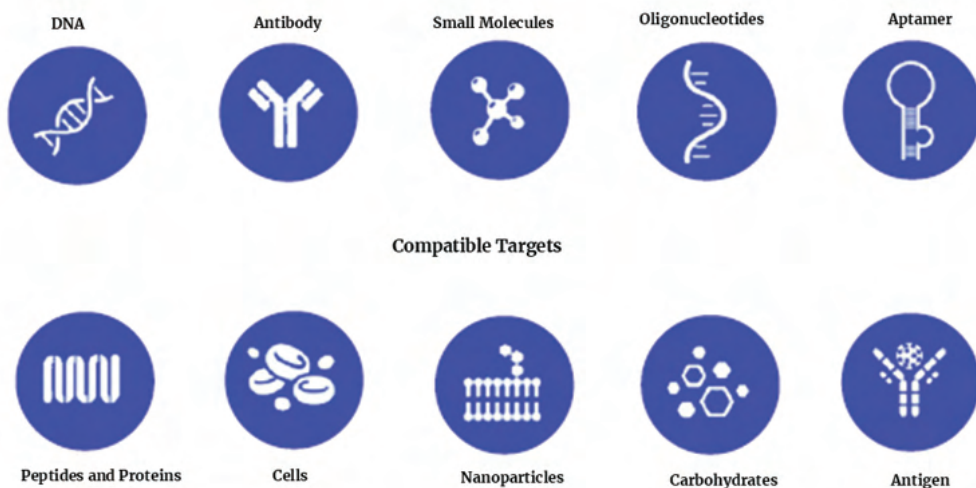


# Product Highlight

## Applications

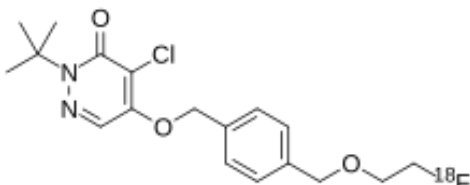
Affinité's Lenseless SPR Systems offer real-time, label-free analysis of molecular interactions in a variety of research applications including –

- **Biosensing**
- **Environmental Testing**
- **Drug Discovery**
- **Biomanufacturing**
- **Bioanalytical Testing and More**



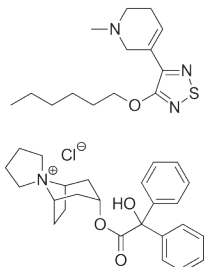
## Sensor Chips/Consumables

Sensor	Surface modified for attachment	Target analytes
Gold	Our gold sensor has a surface modified with thiolated ligands	DNA, RNA, nucleic acid, and aptamer
Carboxyl	Our carboxyl sensor has a surface modified with an amine group on the ligands using EDC/NHS coupling	Antibody, protein, peptide and small molecule
NTA	Our NTA sensor has a surface modified with histidine-tagged ligands	Antibody, protein, peptide and small molecule
Streptavidin	Our streptavidin sensor has a surface modified with biotin-tagged ligands	Antibody, protein, peptide and small molecule
Afficoat	Our proprietary Afficoat sensor has an amine group on the ligands using EDC/NHS coupling	Antibody, protein in cell lysate, serum, plasma, other crude sample and complex matrices
Glass	Our glass sensor has a customized metallic surface	Not applicable

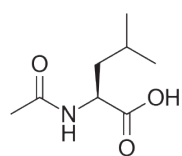


**Flurpiridaz F 18 (Flyrcado)** is a radioactive diagnostic drug used for PET myocardial perfusion imaging (MPI). It is used in adults with coronary artery disease (CAD) to evaluate heart blood flow blockages (myocardial ischemia) and a heart attack (myocardial infarction).

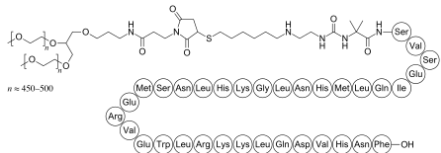
The radioactive Flurpiridaz F 18 binds to heart tissue with biologically active mitochondria. The radioactivity difference seen in PET MPI of a healthy heart compared to an infarcted heart, helps detect heart blockages.



**Xanomeline and trospium chloride (Cobenfy)** treats schizophrenia through two mechanisms-of-action. The active ingredients xanomeline and trospium chloride are muscarinic agonist (selectively targeting M<sub>1</sub> and M<sub>4</sub> receptors in the brain) and muscarinic agonist (blocking muscarinic receptors in peripheral tissues in the brain) respectively.



**Levacetylleucine (Aqneursa)** helps improve functional and neurological symptoms of Niemann-Pick disease type C. It is a modified amino acid with plausible MOA by symptomatic and neurological normalisation of energy metabolism.



**Palopegteriparatide (Yorvipath)** is a parathyroid hormone analog used for the treatment of hyperparathyroidism in adults. It releases PTH (1-34), which temporarily restores physiologic levels of parathyroid hormone, maintaining the balance of calcium and phosphate in the body.

**Lebrikizumab (Ebglyss)** is an IgG4 monoclonal antibody (mAb) that binds to IL-13, for the treatment of atopic dermatitis in adults and children.

# Industry Buzz



## Dive deeper with CATALYSTCue



Want to share your research updates for potential inclusion in the next issue?

Got a burning question or a groundbreaking idea?

Eager to bring Inkarp to your lab?

Host an Inkarp Roadshow and get hands-on experience of our wide range of equipment.

Get in touch with us at [info@inkarp.co.in](mailto:info@inkarp.co.in)



**Scan** here to view  
CATALYSTCue Issue 01

**Do you have expertise you'd like to share? CatalystCue is looking for guest authors! To become a contributor, submit your article proposals to [info@inkarp.co.in](mailto:info@inkarp.co.in)**

Connect with us online

Use **#CATALYSTCue** to spark a conversation about scientific advancements.

For latest news, insights, and discussions in the world of science, follow us on



## **Titramax 1000**

With a shaking orbit of **1.5 mm**, speeds of up to **1,350 rpm**, max. loading capacity of **5kg** and a timer, the **Titramax 1000 features** everything you will ever need!

Storage capacity of up to six multi-well plates

Integrates into the modular incubation system and carries out temperature-controlled processes

Easy loading and removal of the plates